Entanglement in Radiative Cascades

Research Thesis

Submitted in partial fulfillment of the requirements for the degree of
Master of Science in Physics

Eli A. Meirom

Submitted to the Senate of the Technion - Israel Institute of Technology
Nisan 5768 HAIFA April 2008

This research thesis was done under the supervision of Prof. Joseph E. Avron and Prof. D. Gershoni in the Department of Physics

Acknowledgments

I would like to express my gratitude to my supervisors, Prof. Joseph E. Avron and Prof. David Gershoni, for inspiring guidance and constant support. Their scientific knowledge and understanding were invaluable.

The generous financial support of the Technion, NSF and the Russell Berry Nanotechnology Institute is gratefully acknowledged.

I'm thankful to Netanel Linder and Dr. Oded Keneth for their advices and assistance. I cherished the oppretunity I had to work with my wonderful colleague, Gili Bisker.

Finally, I would like to thank my fiancee Michal (Pit) and my family for their support and patience.

Contents

Abstract **1**

List of Symbols **2**

1 Introduction and outline **3**

2 Derivation of the two photons wave function **6**

2.1 Propagator formalism 6

2.2 Propagator identity 8

2.3 The dipole and the rotating wave approximations 9

2.4 Two levels system - Weiskopf-Wigner model 11

2.5 Three levels system 17

2.6 Quadrilateral model 19

3 The polarization density matrix and entanglement distillation **23**

4 The phase of the off diagonal element **28**

4.1 Branching ratios and matrix elements 29

4.2 The role of the complex pole 31

Strong filtering: 31

No filtering: 32

5 Application to quantum dots **35**

6 Comparison with experiment **37**

7 Summary and Conclusions **39**

A Gauge fixing and quantum tomography **40**

List of Figures

1 The excited state $|u\rangle$ can decay via two channels with distinct polarizations, X or Y. The wave function of the photon pair emitted in the cascade is characterized by 3 complex energies, $Z_j = E_j - i\Gamma_j$, $j = x, y, u$. A window of width w indicates the spectral filtering of the emitted photons. 4

2 The integration contour of Eq. 2.4. The contour along $I_\pm$ is along the line $z = k \pm i\eta$. The two integrals are connected at $\pm\infty$. For $t > 0$ the I_- integral can be closed from below (the green contour, each side with length L) and vanishes. 8

3 Radiating system configurations. In Fig. (a) a two levels system is displayed. The emitted photon is x polarized. In Fig (b) a three levels system is depicted and the two emitted photons are x polarized. 12

4 The integration contour I_+ is analytically continued downwards to the second Riemann sheet to include the poles at z_0 and k. The integration loops around the branch cut (in blue) which was shifted by the analytical continuation. 16

5 The square represents the spectral filtering. Only wave numbers (k_1, k_2) in the square are retained. The amplitude is most significant near the diagonal line L_1, along which the energy of the two photons adds up to the initial energy ($k_1 + k_2 = E_u$). E_x and E_y are the energies of the intermediate states. As discussed later on in Sec. 5, s describes the slow drift of the levels. The line L_2 obeys the equation $k_1 + k_2 = E_u + 2s$. 25

6 The photon's detection probability p_w and twice the entanglement measure $|2\rho_{xy}|$, where ρ_{xy} is the off-diagonal element. The plot was drawn for $\Delta/\Gamma \approx 17$, as in Akopian *et al* [1]. For $w \to 0$ the asymptotic values are $|2\rho_{xy}| \to 1$ and $p_w \to 0$ and for $w \to \infty$ the asymptotic values are $|2\rho_{xy}| \to \left(\frac{\Gamma^2}{4(\Delta^2+\Gamma^2)}\right)^{\frac{1}{2}}$ and $p_w \to 1$. The sharp change between these values happens on a scale of $O(\Gamma)$ in the vicinity of the point $w = \Delta$. 27

7 The phase of the integrand is determined by the product of the two complex numbers, represented as arrows, pointing from k_2 to the location of the complex energies Z_ε (blue arrow for Z_x and red arrow for Z_y). The location of k_2 is restricted by the window function W. In figure (a) the levels are detuned and the spectral window is smaller than the detuning. In figure (b) the levels are degenerate and in figure (c) the levels are detuned and the window is larger than the detuning. 33

8 A "phase diagram" for the phase of the off-diagonal element in the density matrix ($\arg(\rho_{xy})$). The widths of transition regions are proportional to the radiative width Γ which is the smallest energy scale in the problem. 34

9 The phase of ρ^f_{xy} as a function of the (centered) normalized spectral window width w/Γ and the detuning Δ/Γ. The line obeys the equation $w = \Delta - 2\Gamma$. For $w, \Delta \gg \Gamma$, for any w which is smaller than $\Delta - 2\Gamma$ the phase does not change appreciably and it is close to 180°. 34

10 The relative "weight" of the density matrix $\rho(s)$. The weight is given by $\Lambda(s) = P(s)Tr(W\rho(s))$. The plot is renormalized to yield $\Lambda(s = 0) = 1$. The plot is obtained with the experimental values as in Sec. 6. 36

11 Comparison between the experimental results of Akopian et al. and the theory. The graph shows a theoretical calculation of the phase as a function of the window, w and the detuning, Δ, both in units of Γ. The calculation uses the experimentally measured parameters w, Δ, Γ and s_0. The uncertainties in these parameters result in an area (rather than a point) indicated by the error bars. The possible theoretical values of the phase are in the area which is bounded by these error bars. These values need to be compared to the experimentally measured phase and error, which is represented in the color bar to the left. 38

Abstract

We study photons which are emitted in a radiative cascade. The emitted photons may have either $\hat{\mathbf{x}}$ or $\hat{\mathbf{y}}$ polarization. In the absence of other degrees of freedom (a "*which path*" information) which indicate the polarization, the photons are entangled in polarization. If there is a partial "*which path*" information, for example, the photons with $\hat{\mathbf{x}}$ polarization are emitted with slightly different wavelength than the photons with $\hat{\mathbf{y}}$ polarization, but the difference between the frequencies is on the same scale as the spectral width of the photons, then the photons are entangled, but not maximally entangled. The entanglement can be distilled by selecting only the photons which have the *which path* ambiguity. We develop a framework to calculate the amplitudes and phases of the density matrix after such filtering. The results can be summarized in a two dimensional "phase diagram", both for the phase and magnitude of the non-diagonal elements of the density matrix. The theory is applied to the quantum tomography of the decay cascade of a biexciton in a semiconductor quantum dot. The effect of inhomogeneous broadening due to fluctuation in the electromagnetic field is discussed in order to facilitate comparison with the experimental measurements.

List of Symbols

symbol	**Meaning**
ρ	Density matrix
Γ	Radiative width
Δ	Detuning
$U(t)$	Time evolution operator
$G(z)$	Propagator
H	Hamiltonian
k	Photon wavenumber
A	Vector potential
$\mathbb{1}$	Identity Operator
$\mathbf{P}$	Momentum operator
QD	Quantum Dot

1 Introduction and outline

In this work we study theoretically the wavefunction and density matrix of the emitted photons in a specific radiative cascade configuration. In this specific configuration, there exists an upper level $|u\rangle$ and a ground state $|d\rangle$. From the initial, upper level, a radiative cascade is possible via two intermediate states, $|x\rangle$ and $|y\rangle$. This is shown in Fig. 1. The upper level may decay to the intermediate state $|\varepsilon\rangle$, $\varepsilon = x, y$, while emitting a photon with $\hat{\boldsymbol{\varepsilon}}$ polarization. Then, another photon with $\hat{\boldsymbol{\varepsilon}}$ polarization is emitted after the level $|\varepsilon\rangle$ has decayed to the ground state $|d\rangle$. In this specific configuration, the final wavefunction $|\psi_2\rangle$ of the two photons is then a superposition of the photons having both $\hat{\mathbf{x}}$ polarization with the state of the photons having both $\hat{\mathbf{y}}$ polarization.

If the photons with $\hat{\mathbf{x}}$ polarization are identical to the photons with $\hat{\mathbf{y}}$ polarization in the remaining degrees of freedom, then the state ρ will be maximally entangled. This situation is sometimes described as the emitted photons containing no *which path* information or ambiguity. If the photons with $\hat{\mathbf{y}}$ polarization are clearly distinguishable from the photons with $\hat{\mathbf{x}}$ polarization then the density matrix will be a mixed state. It may happen that the photons with $\hat{\mathbf{x}}$ polarization photons are *partially* distinguishable from the photons with $\hat{\mathbf{y}}$ polarization. Such a situation may happen when the difference between the photon's frequencies is comparable to the radiative width of the photons. In this case, the density matrix is entangled, but not maximally entangled.

We shall consider here the 2-qubits state describing the polarization of two photons obtained from a decay cascade with a partial *which path* ambiguity, as in Fig. 1. As the density matrix will be partially entangled, the entanglement might be poor. However, entanglement can be distilled by filtering [1], and selecting only photons with *which path* ambiguity, a processed we call "spectral filtering" .

We describe a theoretical framework for computing the distilled 2-qubit density matrix using only quantities that can be measured independently such as energies and life-times of the quantum states. We derive the behavior of the density matrix elements (phase and magnitude) under such distillation.

It is not clear if and what physical information is encoded in the phases of the density matrix (the phases of the non-diagonal elements) and whether the information is intrinsic to the cascade or rather a feature of the distillation procedure. The phases measured in [1, 2, 3] have, so far, not been explained by a theoretical model. Our work will focus on the understanding of the phases in the density matrix and on the physical information they contain. We shall describe how these entries are computed (in Sec. 2) and pay particular

attention to what governs the phase of the off-diagonal element in the matrix (in Sec. 3-5).

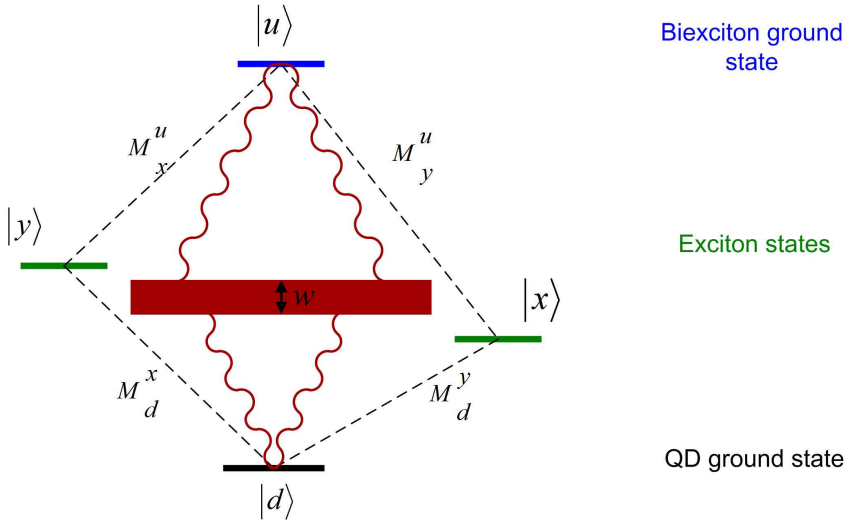

Figure 1: The excited state $|u\rangle$ can decay via two channels with distinct polarizations, X or Y. The wave function of the photon pair emitted in the cascade is characterized by 3 complex energies, $Z_j = E_j - i\Gamma_j$, $j = x, y, u$. A window of width w indicates the spectral filtering of the emitted photons.

The outline of this thesis is as follows. In Sec. 2 we derive the two photons' wavefunction $|\psi_2\rangle$. We show that the wave function has a universal functional form, Eqs. (2.72-2.74), parameterized by three complex phenomenological constants $Z_j = E_j - i\Gamma_j$, $j = x, y, u$ (we have chosen the ground state to have $E_d = 0$). E_j is the energy of the j-th state and Γ_j is its width[1]. Γ is the radiative width, which is the smallest energy scale in the problem. (For concreteness, we set $\Gamma = \Gamma_x = \Gamma_y = \Gamma_u/2$, as is appropriate for a biexciton decay.)

In the next section, the polarization density matrix and the distillation process is presented. The phases of the non-diagonal matrix elements are derived in Sec. 4, and can be seen qualitatively in Fig. 8. In order to compare the theoretical prediction for the phase with the experimental result of Akopian *et al.* [1], we discuss a specific effect in quantum dots which may have hindered the previous (expected) results. We show in Sec. 5 that this effect, the slow and random change in the level's energies, does not harm the previous results appreciably due to the spectral filtering. We quantify its effect on the measured density matrix and compare it with the experimental results in Sec. 6. We

[1]The common convention [4] replaces our Γ by $\Gamma/2$.

show that the experimental result is within one standard deviation from the theoretical prediction.

A remark about the notation. This thesis is written in the convention $\hbar = c = 1$ and $e = \sqrt{\alpha} = \sqrt{137^{-1}}$. In some instances we will write these constants explicitly.

2 Derivation of the two photons wave function

Consider a radiating system, say a quantum dot, which decays while emitting two photons. The wave function of the photon pair is necessarily of the form

$$|\psi_2(t)\rangle = \sum_{\varepsilon=x,y} \int dk_1 dk_2 \lambda_\varepsilon \alpha_\varepsilon(k_1,k_2) e^{-i(k_1+k_2)t} \; |k_1,k_2\rangle \otimes |\hat{\varepsilon}\hat{\varepsilon}\rangle \tag{2.1}$$

ε denotes the polarization. λ_ε are the branching ratios for the two decay modes. Our goal in this section is to derive $\alpha_\varepsilon(k_1,k_2)$ assuming at $t=0$ the radiating system was in the initial state $|u\rangle$ (see Fig. 1) and no photons were present. We will follow and elaborate on the procedures mentioned in Cohen-Tannoudji *et al.* [4], mainly in Sec. 2.1 and Sec. 2.2.

As this section is somewhat technical, we indicate the main milestones. First, we write the evolution operator $U(t)$ as an integral over a propagator (Sec. 2.1). Then we derive in Sec. 2.2 a useful propagator identity, Eq. 2.15. A simple form for the interaction V between the electromagnetic field and the radiating system, Eqs. (2.21,2.22) is obtained by using the dipole and the rotating wave approximations. Using this form, we apply the propagator identity in Sec. 2.4 to a simple model of a radiative cascade in a two-levels system. This allows us to calculate explicitly the propagator (the integrand). We generalize the previous result to a cascade from a three levels system (Sec. 2.5) and to a "quadrilateral" configuration, similiar to the levels diagram in quantum dots (Sec. 2.5). This will be the desired, final result for this section, Eqs.(2.72-2.74).

The results of this section will be briefly presented in Sec. 3, and if desired the reader may skip to the next section.

2.1 Propagator formalism

The interaction of matter with electromagnetic fields may be described by the Hamiltonian

$$H = H_0 + V \tag{2.2}$$

where H_0 is the hamiltonian of the radiating system and the electromagnetic field and V describes the interaction of the electromagnetic field with the radiating system. Define for a general projection P on an eigenspace of H_0 the operator and any operator B:

$$G(B,P;z) \triangleq P\frac{1}{z-P(H_0+B)P}P \tag{2.3}$$

We can write the evolution operator $U(t)$ as

$$U(t) = \frac{1}{2\pi i}\int e^{-izt}\frac{1}{z-H}dz = \frac{1}{2\pi i}\int e^{-izt}G(V,\mathbb{1};z)dz \tag{2.4}$$

The integration along the contour $(I_+ + I_-)$ encircles the eigenvalues of H, as depicted in Fig. 2. Note that $G(V, P; z)$ is the propagator for the full hamiltonian, but restricted to the eigenspace P, so $G(z) \triangleq G(V, \mathbb{1}; z)$ is the complete propagator. Also, $G(0, \mathbb{1}; z)$ is the unperturbed propagator.

We use $|k_i, k_j ...\rangle$ to indicate the state of the photons and $|s\rangle$ for the state of the radiating system. A more compact notation is sometimes used and we write the total state as $|k_i, k_j ...; s\rangle$. If the polarization of the photons is also relevant, we use a third index $\hat{\boldsymbol{\varepsilon}}$ and write $|k_i, k_j ...; s; \hat{\boldsymbol{\varepsilon}}\rangle$.

We are interested in the two photons wavefunction. In order to derive it, we need to calculate $\langle k_1, k_2; d| U(t) |0; u\rangle$. Eq. 2.4 insturcts us to first evaluate $\langle k_1, k_2; d| G(V, \mathbb{1}; z) |0; u\rangle$.

The integrand's matrix element $\langle k_1, k_2; d| G(V, \mathbb{1}; z) |0; u\rangle$, viewed as a function of z, is analytic everywhere bar the real axis, and for $t > 0$ the integral I_- vanishes by the following contour deformation: We close the contour from below, by the lines $I_1 + I_2 + I_3$, all of length L (Fig. 2). As there are no poles in the lower half plane, the integral along this contour vanishes, and therefore $I_- = I_1 + I_2 + I_3$. Choose $L \gg E_u$. As

$$\langle k_1, k_2; d| \frac{1}{z - H} |0; u\rangle \approx \frac{1}{z - E_u} \tag{2.5}$$

and either $\mathbb{I}m\ z = L$ (as along the I_2 line) or $\mathbb{R}e\ z = L/2$ (Along the line I_1 and I_3) we can approximate:

$$O\left(\langle k_1, k_2; d| \frac{1}{z - H} |0; u\rangle\right) = O\left(\frac{1}{L}\right) \tag{2.6}$$

Therefore, the I_2 integral can be approximated

$$\begin{aligned} I_2 &= \frac{1}{2\pi i} \int e^{-izt} \langle k_1, k_2; d| \frac{1}{z - H} |0; u\rangle \\ &\approx L \frac{e^{-Lt}}{L} = e^{-Lt} \end{aligned} \tag{2.7}$$

The integral along the line I_1 (and I_3 in a similar way) is approximated by

$$\begin{aligned} I_1 &\approx \int_0^L dx \frac{e^{-xt}}{L} \\ &= \frac{1 - e^{-Lt}}{Lt} \approx \frac{1}{Lt} \end{aligned} \tag{2.8}$$

For a given t we'll choose L large enough so all these integrals are small to conclude that $I_1, I_3 \approx 0$. Hence, for $t > 0$ the only contribution to the integral in Eq. 2.4 is along the line I_+.

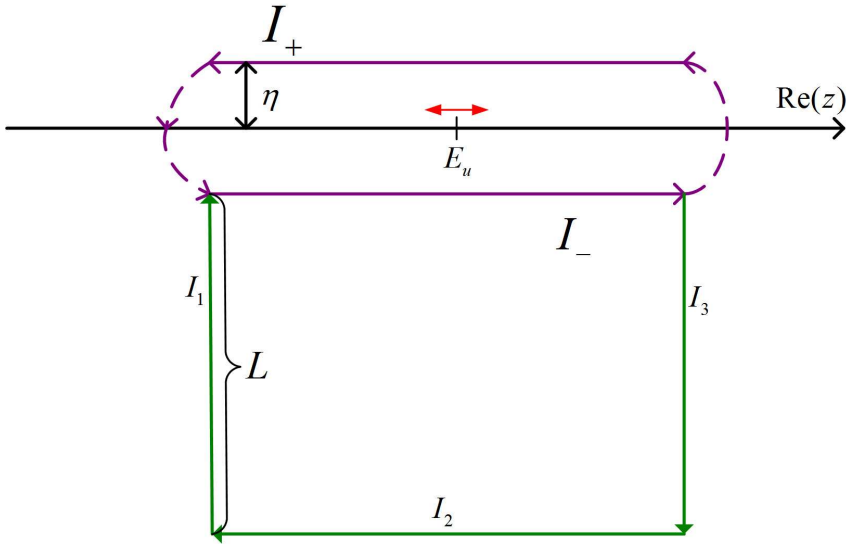

Figure 2: The integration contour of Eq. 2.4. The contour along $I_\pm$ is along the line $z = k \pm i\eta$. The two integrals are connected at $\pm\infty$. For $t > 0$ the I_- integral can be closed from below (the green contour, each side with length L) and vanishes.

2.2 Propagator identity

Define $Q = \mathbb{1} - P$. If we multiply the identity

$$(z - H)G(z) = \mathbb{1} \tag{2.9}$$

from the right by Q and from the left by P, and insert the $P + Q = \mathbb{1}$ between $z - H$ and $G(z)$, we get

$$\begin{aligned} 0 &= Q(z - H)(P + Q)G(z)P \\ &= -QVP \cdot PG(z)P + Q(z - H)Q \cdot QG(z)P \end{aligned} \tag{2.10}$$

since $P(z - H_0)Q = 0$. We obtained

$$\begin{aligned} QG(z)P &= (Q(z - H)Q)^{-1}QVPPG(z)P \\ QG(z)P &= Q(Q(z - H)Q)^{-1}Q \cdot QVP \cdot PG(z)P \\ QG(z)P &= G(V, Q; z)VPG(z)P \end{aligned} \tag{2.11}$$

Likewise, if we multiply Eq. 2.9 from the left and right by P:

$$\begin{aligned} P &= P(z-H)(P+Q)G(z)P \\ &= -PVQ\cdot QG(z)P + P(z-H)P\cdot PG(z)P \\ &= -PVQ\cdot G(V,Q;z)V\cdot PG(z)P + P(z-H)P\cdot PG(z)P \\ &= P(-V\cdot G(V,Q;z)V + z - H)P\cdot PG(z)P \\ &= P(z-H_0-V-V\cdot G(V,Q;z)V)P\cdot PG(z)P \end{aligned} \tag{2.12}$$

If we define

$$R^Q(z) = V + VQ\cdot G(V,Q;z)V = V + VQ\frac{1}{z-Q(H_0+V)Q}QV \tag{2.13}$$

Then

$$PG(z)P = P\frac{1}{z-P(H_0+R^Q(z))P}P \tag{2.14}$$

Substituting this in Eq. 2.11, we obtain the next identity,

$$(\mathbb{1}-P)G(z)P = G(V,\mathbb{1}-P;z)VG(R^{\mathbb{1}-P},P;z) \tag{2.15}$$

This will be our main tool in deriving the emitted photons wave function.

2.3 The dipole and the rotating wave approximations

The interaction between the radiating system and the electromagnetic field originates from the kinetic energy term, $(\mathbf{P}-q\mathbf{A})^2/2m$, in the hamiltonian. $\mathbf{A}$ is the vector potential and $\mathbf{P}$ is the particle momentum.

Consider a few-levels radiating system, which emits photons. We assume that due to the cavity structure the emitted photons propagate along the $\hat{\mathbf{z}}$ axix. The polarization ε is then a vector in the $x-y$ plane, and we choose as the polarization basis as the $\hat{\mathbf{x}}$ and $\hat{\mathbf{y}}$ polarizations. The interaction V can be written in the Coulomb gauge as:

$$V = \frac{\mathbf{P}\cdot q\mathbf{A}}{m} = \sum_k \frac{a^\dagger_{k,\varepsilon} q e^{-ikz}}{m}\mathbf{P}\cdot\varepsilon + h.c \tag{2.16}$$

since $[\mathbf{A},\mathbf{P}]=0$ in the Coulomb gauge. In writing Eq. 2.16, we have neglected a term of order $O(\mathbf{A}^2)$. Such a term also appears in

$$\mathbf{P}\cdot q\mathbf{A} = (m\mathbf{v}+q\mathbf{A})\cdot q\mathbf{A} \approx mq\mathbf{v}\cdot\mathbf{A} \tag{2.17}$$

and we will neglect it and approximate

$$\mathbf{P} = (m\mathbf{v} + q\mathbf{A}) \approx m\mathbf{v} \tag{2.18}$$

In order to improve our understanding of V, we simplify the matrix elements of the operator $e^{-ikz}\mathbf{P}\cdot\varepsilon$. In most of the radiating systems, as in quantum dots, the emitted photons wavelength is much longer than the dimensions of the radiating system. Since $kz \ll 1$ we can approximate:

$$e^{-ikz} \approx 1 \tag{2.19}$$

This is known as the dipole approximation. Using Eq. 2.18 and the commutation relation $m[H_0, \mathbf{r}] = im\dot{\mathbf{r}} = im\mathbf{v} = i\mathbf{P}$:

$$\begin{aligned} \langle j|\, e^{-ikz}\mathbf{P}\cdot\varepsilon\,|j'\rangle &= \langle j|\,\mathbf{P}\cdot\varepsilon\,|j'\rangle = -\langle j|\, mi[H_0, \mathbf{r}\cdot\varepsilon]\,|j'\rangle \\ &= -i(E_j - E_{j'})m\,\langle j|\,\mathbf{r}\cdot\varepsilon\,|j'\rangle \end{aligned} \tag{2.20}$$

where $\mathbf{r}\cdot\varepsilon$ is the coordinate in the ε direction and m is the mass of the particle. This expression also indicate that all the diagonal elements of V vanish (if there is no degeneracy). This allows us to write Eq. 2.16 in the form:

$$V = \sum g_{jj'}\,|j\rangle\,\langle j'|\,a^{\dagger}_{k,\varepsilon} + h.c \tag{2.21}$$

where

$$g_{jj'} = i(E_j - E_{j'})q\,\langle j|\,r_{\varepsilon}\,|j'\rangle\,. \tag{2.22}$$

This expression is propotional to the dipole moment, hence the term "the dipole approximation". In fact, by a gauge transformation [4, 5] one can express the interaction V, given in 2.16, as a dipole interaction term $\mathbf{d}\cdot\mathbf{E}$.

We can write Eq. 2.16 as an nXn matrix where n is the number of levels, in the following manner. Each level has a representation in coordinate space (or momentum space). Therefore, any operator O is an nXn matrix, with entries $\langle m|\,O\,|n\rangle$. For example, for a two levels system, denoted $|0\rangle$ and $|1\rangle$, the $\mathbf{r}\cdot\varepsilon$ operator is given in the form:

$$\mathbf{r}\cdot\varepsilon = \begin{pmatrix} \langle 0|\,\mathbf{r}\cdot\varepsilon\,|0\rangle & \langle 1|\,\mathbf{r}\cdot\varepsilon\,|0\rangle \\ \langle 0|\,\mathbf{r}\cdot\varepsilon\,|1\rangle & \langle 1|\,\mathbf{r}\cdot\varepsilon\,|1\rangle \end{pmatrix} \tag{2.23}$$

If second quantization is used for the particles in the radiating system one use $\mathbf{P} = \sum_{m,n}\langle m|\,P\,|n\rangle\,b^{\dagger}_m b_n$ where b_n is annihilation operator of a particle in mode n. The same form for the potential (Eq. 2.21) can be derived, where the states $|j\rangle\,, |j'\rangle$ are in Fock

space. Assume, for example, $|j'\rangle = |vac\rangle$ and $|j\rangle = b_c^\dagger b_v$ where the mode v is in the valence band and c is a mode in the conductance band. Then the matrix element of V between the states $|j\rangle$ and $|j'\rangle$ describes the emission of a photon by the anhilition of an exciton (an electron-hole pair).

Note that the operator V contains terms that are not energy-conserving, for example, an excitation of the radiating system *and* a creation of a photon, which in Eq. 2.21 will be a term proportional to $a_{k,\varepsilon}^\dagger |j'\rangle \langle j|$ with $E_j < E_{j'}$. We will neglect those terms (the rotating wave approximation).

Under these approximations, the V operator induces a transition between levels while creating (or destroying) one photon.

Define the number of excitations in the system (electromagnetic field+radiating system) as the sum of the number of photons present (excitations of the electromagnetic field) and the number of excitations of the radiating system (n if the radiating system in the $n+1$ excited state). Then, the interaction V, Eq. 2.16, conserves the number of excitations. Since the non-interacting hamiltonian

$$H_0 = \sum_i E_i |i\rangle \langle i| + \sum_k \hbar k a_{k,\varepsilon}^\dagger a_{k,\varepsilon} \tag{2.24}$$

also conserves this quantity, this conserved number breaks the complete hamiltonian into a block matrix, each block representing a different number of excitations. It it enough to discuss the evolution in time for a given number of excitations.

Before applying these general results to the radiating system of our concern, as depicted in Fig. 1, it is instructive to discuss some simpler cases. We'll first treat the problem of radiating system composed of two levels, in which we will deploy most of the tools of the trade. This will make the transition to a three levels system fairly straightforward. The next and last step to the quadrilateral radiating model as described in Sec. 1 is then immediate.

2.4 Two levels system - Weiskopf-Wigner model

Consider a two-levels system, as depicted in Fig 3(a). We'll name the upper level as $|u\rangle$ and the lower as $|x\rangle$ for reasons which will become clear later. In such a configuration, Eqs. (2.21,2.22) contain only one coupling constant $g_1 = g_{xu}$. In the following discussion, we'll restrict ourself to the subspace of one excitation in the system, as defined in the previous section.

In order to find the matrix elements of the time evolution operator, $\langle k_1; x| U(t) |0; u\rangle$, Eq. 2.4 instructs us to find first the propagator's matrix elements, $\langle k_1; x| G(V, \mathbb{1}; z) |0; u\rangle$.

Define P_i as a projection on the eigenspace of H_0 which contains exactly i photons, for example

$$P_1 \triangleq \sum_{k_i} |k_i; x\rangle \langle k_i; x| \tag{2.25}$$

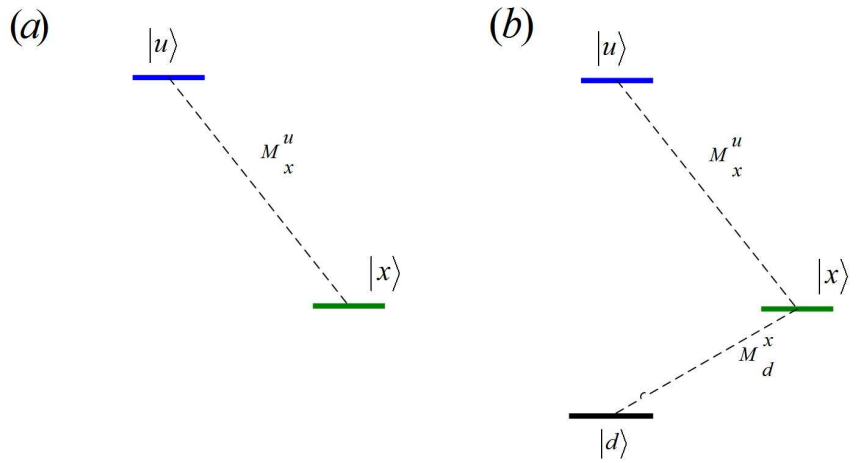

Figure 3: Radiating system configurations. In Fig. (a) a two levels system is displayed. The emitted photon is x polarized. In Fig (b) a three levels system is depicted and the two emitted photons are x polarized.

As was seen in the previous subsection, the interaction V has non-vanishing elements only between eigenspaces with different number of photons (specifically, only between eigenspaces which contain exactly one more or one less photons), that is, V obeys

$$P_i V P_i = 0 \tag{2.26}$$

Substituting this in Eq. 2.3, we derive

$$G(V, P_i; z) = G(0, P_i; z) \tag{2.27}$$

Also, $G(A, P_i; z),\ A = V, 0$ has vanishing elements between eigenvectors which belong to subspaces with a different number of photons,

$$P_j G(A, P_i; z) = G(A, P_i; z) P_j = 0 \qquad i \neq j \tag{2.28}$$

Using these identities with Eq. 2.15 allows us to write

$$\begin{aligned}\langle k_1; x|\, G(V, \mathbb{1}; z)\, |0; u\rangle &= \langle k_1; x|\, P_1 G(V, \mathbb{1}; z) P_0\, |0; u\rangle \\ &= \langle k_1; x|\, G(V, P_1; z) V G(R^{\mathbb{1}-P_0}, P_0; z)\, |0; u\rangle \\ &= \langle k_1; x|\, G(0, P_1; z) V G(R^{P_1}, P_0; z)\, |0; u\rangle\end{aligned} \tag{2.29}$$

We can evaluate this expression precisely. Inserting the identity operator for the space with one excitation $\mathbb{1} = P_0 + P_1$ and using Eqs. 2.26-2.28 we write

$$\begin{aligned}\langle k_1; x|\, G(0, P_1; z) V G(R^{P_1}, P_0; z)\, |0; u\rangle &= \langle k_1; x|\, G(0, P_1; z) \mathbb{1} V \mathbb{1} G(R^{P_1}, P_0; z)\, |0; u\rangle \\ &= \langle k_1; x|\, G(0, P_1; z) P_1 V P_0 G(R^{P_1}, P_0; z)\, |0; u\rangle \\ &= \sum_{k_i} \langle k_1; x|\, G(0, P_1; z)\, |k_i; x\rangle \langle k_i; x|\, V\, |0; u\rangle \\ &\quad \times \langle 0; u|\, G(R^{P_1}, P_0; z)\, |0; u\rangle\end{aligned} \tag{2.30}$$

where we noted that P_u is an eigenspace of $G(R^{P_1}, P_u; z)$. The G terms can be expressed explicitly.

$$\begin{aligned}\langle u|\, G(R^{P_1}, P_0; z)\, |u\rangle &= \langle u|\, \frac{1}{z - |u\rangle \langle u|\, (H_0 + R^{P_1})\, |u\rangle \langle u|}\, |u\rangle \\ &= \frac{1}{z - E_u - \langle u|\, R^{P_1}\, |u\rangle}\end{aligned} \tag{2.31}$$

$$\begin{aligned}\langle k_1; x|\, G(0, P_1; z)\, |k_i; x\rangle &= \langle k_1, x|\, \frac{1}{z - P_1 H_0 P_1}\, |k_i; x\rangle \\ &= \langle k_1; x|\, \frac{1}{z - (E_x + k_m) \sum_{k_m} |k_m; x\rangle \langle k_m; x|}\, |k_i; x\rangle \\ &= \langle k_1; x|\, \frac{1}{z - k_1 - E_x}\, |k_i; x\rangle\, \delta_{i1}\end{aligned} \tag{2.32}$$

we deploy these results in Eq. 2.30 and obtain:

$$\langle k_1; x|\, G(z)\, |0; u\rangle = \langle k_1; x|\, V\, |0; u\rangle \prod_{i=1}^{2} \frac{1}{z - E_i - R_i(z)} \tag{2.33}$$

where we have labeled:

$$\begin{aligned} E_1 &= E_u & R_1(z) &= \langle u|\, R^{P_1}\, |u\rangle \\ E_2(k) &= k_1 + E_x & R_2(z) &= 0 \end{aligned} \tag{2.34}$$

The next step is to evaluate $R_1(z)$.

$$\begin{aligned} R_1(z) &= \langle u| R^{P_1} |u\rangle \\ &= \langle u| V(1 + P_1 \frac{1}{z - P_1(H_0 + V)P_1} P_1 V) |u\rangle \\ &= \langle u| V P_1 \frac{1}{z - P_1 H_0 P_1} P_1 V |u\rangle \\ &= \sum_{k_i} \frac{|\langle k_i; x| V |u\rangle|^2}{z - k_i - E_x} = \sum_{k_i} \frac{|g_1|^2}{z - k_i - E_x} \end{aligned} \tag{2.35}$$

where we used Eq. 2.26.

A further simplification is possible by the use of

$$\frac{1}{x + i\eta} = P.V\left(\frac{1}{x}\right) - i\pi\delta(x) \tag{2.36}$$

to write:

$$\begin{aligned} R_1(z) &= \sum_{k_i} \frac{|g_1|^2}{z - k_i - E_x} \\ &= \fint dk \frac{|g_1|^2}{Re(z) - k - E_x} dk - i\pi |g_1|^2 \\ &\triangleq \Upsilon(z) - i\Gamma(z) \end{aligned} \tag{2.37}$$

It is important to notice that $\Gamma(z) = \pi|g_1|^2$ is a positive constant, which we'll denote by Γ. Thus, we obtained the matrix element of the time evolution operator:

$$\begin{aligned} \langle k_1; x| U(t) |0; u\rangle &= \frac{1}{2\pi i} \int dz e^{-izt} \langle k_1; x| G(z) |0; u\rangle \\ &= \frac{\langle k_1; x| V |0; u\rangle}{2\pi i} \int dz e^{-izt} \prod_{i=1}^{2} \frac{1}{z - E_i(k) - R_i(z)} \end{aligned} \tag{2.38}$$

Where the integration is performed along I_+ (Fig. 4).

Our goal is now to integrate Eq. 2.38 to obtain the emitted photon amplitude, Eq. 2.44. In order to do that, a few more approximations are needed. The next approximation we introduce is to observe that both $\Upsilon(z)$ and Γ are small, since they are of order $O(V^2)$. Hence, there is a pole in the vicinity of E_1, which we denote by z_1, and a pole on the real axis in $E_2(k)$. We'll deform the contour as displayed in Fig. 4. The integrals along the arcs vanish and we are left with contributions from the poles and from the integrals on the two sides of the branch cut. Here, we'll introduce a second approximation, and

we'll observe only long times, that is, at times such that $\Gamma t \gg 1$. This approximation will allow us to neglect the contribution of the pole at z_1, since it is diminished by a factor $e^{-\Gamma t}$. The integral on the two side of the cut is the integral on the difference between the analytic continuation of the propagator on the upper half plane and the propagator as defined on the lower half plane. A similar analysis for the propagators on the first Riemann sheet shows the difference between the two propagators (on the first and on the second Riemann sheets) is the sign of the imaginary part of $R_1(z)$, that is, Γ. The branch cut can be shifted to be along the line $Re(z) = 0$. The relevant wavevectors are such that $k_1 \approx E_u$ and along this line $|z - E_u| \approx |z - k_1| < E_u$. Since $R_1(z)$ is small the integral of Eq. 2.38 along the branch cut is then given in the form

$$\begin{aligned} \int dz e^{-izt} \frac{1}{z - k_1} \quad & \left(\frac{1}{z - E_u - R_1(z)} - \frac{1}{z - E_u - \overline{R_1}(z)}\right) \\ & = 2 \int dz e^{-izt} \frac{1}{z - k_1} \frac{\Gamma(z)}{|z - E_u - R_1(z)|^2} \leq \frac{\Gamma(z_0)}{E_u^3 t}. \end{aligned} \tag{2.39}$$

We used the fact that $\Gamma(z)$ is of the order of $\Gamma(z_0)$. In contrast, the contribution of the pole on the real axis to the relevant wavevectors (as will be shown later, Eq. 2.43) scales like Γ^{-1}. The ratio is of the order

$$\left(\frac{\Gamma}{E_u}\right)^2 \frac{1}{E_u t} \tag{2.40}$$

From Eq. 2.35 Γ is of the order V^2/E_u. Since the energy of the excited state, the electrostatic energy and the photon's energy are of the same magnitude $e^2/r \approx \hbar w \approx E_u$, the ratio in the last line is:

$$\begin{aligned} \frac{\Gamma}{E_u} & \approx V^2 \frac{1}{E_u^2} \approx (er \cdot E)^2 \frac{1}{E_u^2} \approx \left(e \frac{e^2}{E_u}\right)^2 \frac{\hbar\omega}{dv} \frac{1}{E_u^2} \\ & = \frac{e^6}{E_u^4} \frac{\hbar w^4}{(\hbar c)^3} = \alpha^3 \end{aligned} \tag{2.41}$$

where $dv = \lambda^3$ is the volume of the electromagnetic field[2]. We conclude that the integral along the sides of the branch cut has a meaningful contribution only at times,

$$t \approx E_u \left(\frac{\Gamma}{E_u}\right)^2 \approx 10^6 \Gamma \tag{2.42}$$

that is, long after the decay, and we neglect the contribution of this integral.

[2]This result can also be obtained by rescaling the radiating system coordiante and a rescaling differently the photon's coordinates (the wavevectors) [6].

We have derived a non-pertubative expression for the emitted photon wave function:

$$\begin{aligned}\langle k_1; x|\, U(t)\, |0; u\rangle &= e^{-ik_1 t}\frac{\langle k_1; x|\, V\, |0; u\rangle}{k_1 - E_1 - R_1(z_0)} \\ &= e^{-ik_1 t}\frac{\langle k_1; x|\, V\, |0; u\rangle}{k_1 - E_u - \Upsilon(z_0) + i\Gamma} \\ &= e^{-ik_1 t}\frac{\sqrt{\Gamma_u/\pi}}{k_1 - E_u - \Upsilon(z_0) + i\Gamma}\end{aligned} \tag{2.43}$$

Thus we have obtained a universal form for the emitted photon in a radiative cascade of a two level system. This universal form requires two phenomenological parameters, E_u, the energy of the higher level (redefined to include the Lamb shift $\Upsilon(z_0)$) and the radiative width of the level, Γ_u. We can write this two parameters as one complex number Z_u and write the universal form as [4]:

$$A(k, Z_u) = \frac{\sqrt{\Gamma_u/\pi}}{|k| - Z_u}, \quad Z_u = E_u - i\Gamma_u \tag{2.44}$$

It is important to remember that in Eq. 2.44 the expression $\sqrt{\Gamma_u/\pi}$ is just the coupling constant which correspond to appropriate transition, that is:

$$\sqrt{\Gamma_u/\pi} = g_1 \tag{2.45}$$

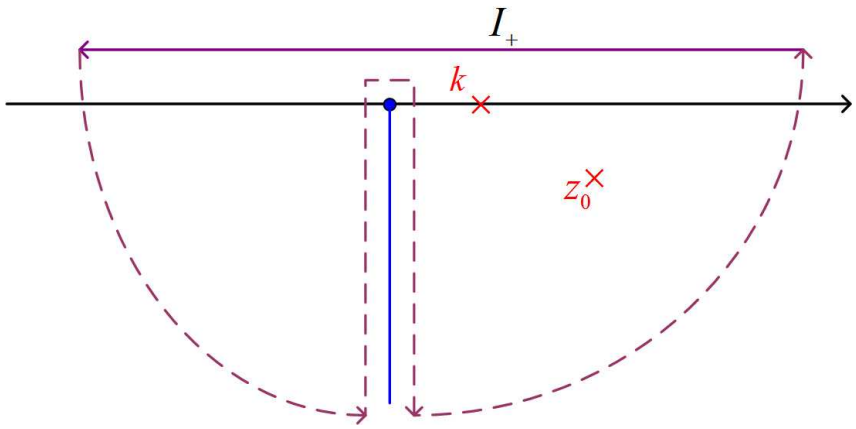

Figure 4: The integration contour I_+ is analytically continued downwards to the second Riemann sheet to include the poles at z_0 and k. The integration loops around the branch cut (in blue) which was shifted by the analytical continuation.

2.5 Three levels system

Let us now consider a three levels radiating system, which is schematically shown in Fig. 3(b). The unperturbed hamiltonian is as in Eq. 2.24, but now the summation is over three levels $i = u, x, d$, and we restrict ourselves to the subspace of three excitations. We'll set $E_d = 0$. Since there are two possible transitions, there are two coupling constants in Eqs. (2.21,2.22). We'll set $g_1 = g_{xu}$ and $g_2 = g_{dx}$. As before, the interaction of the electromagnetic field with the radiating system can be written (ignoring the polarization for now) in the form

$$V = \sum_{k_1} g_1 \left|E_x; k_1\right\rangle \left\langle E_u\right| + \sum_{k_1,k_2} g_2 \left|E_d; k_1, k_2\right\rangle \left\langle E_x; k_1\right| + h.c. \tag{2.46}$$

We'll follow the path of the previous subsection. The identity operator (in the subspace of three excitations) is now

$$\mathbb{1} = P_0 + P_1 + P_2 \tag{2.47}$$

and by the use of Eqs.(2.15, 2.26-2.28), the fact that $|u\rangle$ is an eigenvector of $G(R^{P_1+P_2}, P_0; z)$ and $|k_1, k_2\rangle$ is an eigenvector of the $G(0, P_2; z)$ (as it is just the propagator of the free hamiltonian) we obtain:

$$\begin{aligned}
\left\langle k_1, k_2; d\right| G(z) \left|0; u\right\rangle &= \left\langle k_1, k_2; d\right| G(V, P_2 + P_1; z) V G(R^{P_1+P_2}, P_0; z) \left|0; u\right\rangle \\
&= \left\langle k_1, k_2; d\right| G(0, P_2; z) V G(R^{P_2}, P_1; z) V G(R^{P_1+P_2}, P_0; z) \left|0; u\right\rangle \\
&= \left\langle k_1, k_2; d\right| G(0, P_2; z) V \mathbb{1} G(R^{P_2}, P_1; z) \mathbb{1} V \mathbb{1} G(R^{P_1+P_2}, P_0; z) \left|0; u\right\rangle \\
&= \left\langle k_1, k_2; d\right| G(0, P_2; z) V P_1 G(R^{P_2}, P_1; z) P_1 V P_0 G(R^{P_1+P_2}, P_0; z) \left|0; u\right\rangle \\
&= \sum_{k_i} \left\langle k_1, k_2; d\right| G(0, P_2; z) V P_1 G(R^{P_2}, P_1; z) \left|k_i; x\right\rangle \\
&\quad \times \left\langle k_i; x\right| V P_0 G(R^{P_1+P_2}, P_0; z) \left|0; u\right\rangle
\end{aligned} \tag{2.48}$$

The first term describes the evolution of a two levels system, x and d, with a photon (with either $k_i = k_1$ or $k_i = k_2$) present in the background. We shall treat the symmetrization later, and assume for now that $k_i = k_1$.

Let us discuss the second term of Eq. 2.48.

$$\begin{aligned}
\left\langle k_i; x\right| V P_0 G(R^{P_1+P_2}, P_0; z) \left|0; u\right\rangle &= \left\langle k_i; x\right| V \left|0; u\right\rangle \left\langle 0; u\right| G(R^{P_1+P_2}, P_0; z) \left|0; u\right\rangle \\
&= g_1 \left\langle 0; u\right| \frac{1}{z - \left|0; u\right\rangle \left\langle 0; u\right| (H_0 + R^{P_1+P_2}) \left|0; u\right\rangle \left\langle 0; u\right|} \left|0; u\right\rangle \\
&= g_1 \frac{1}{z - \left\langle 0; u\right| (H_0 + R^{P_1+P_2}) \left|0; u\right\rangle} \\
&= g_1 \frac{1}{z - E_u + \left\langle 0; u\right| R^{P_1+P_2} \left|0; u\right\rangle}
\end{aligned} \tag{2.49}$$

Now, by the use of $P_i V P_0 = P_i V |u\rangle \langle u| = 0$ for $i \neq 1$ and Eq. 2.26

$$\begin{aligned}
\langle 0;u| R^{P_1+P_2} |0;u\rangle &= \langle u| V(1 + (P_1+P_2)\frac{1}{z-(P_1+P_2)(H_0+V)(P_1+P_2)}(P_1+P_2)V) |0;u\rangle \\
&= \langle 0;u| VP_1 \frac{1}{z-(P_1+P_2)(H_0+V)(P_1+P_2)} P_1 V |0;u\rangle \\
&= \langle 0;u| VP_1 \frac{1}{z-P_1(H_0+V)P_1} P_1 V |0;u\rangle \\
&= \langle 0;u| VP_1 \frac{1}{z-P_1 H_0 P_1} P_1 V |0;u\rangle \\
&= \sum_{k_j} \frac{|g_1|^2}{z-k_j-E_x}
\end{aligned} \tag{2.50}$$

The results of the previous section can be applied to obtain

$$\begin{aligned}
\langle k_1,k_2| G(z) |u\rangle &= \langle k_1,k_2;d| V |k_1;x\rangle \langle k_1;x| V |0;u\rangle \prod_{i=1}^{3} \frac{1}{z-E_i-R_i(z)} \\
&= g_1 g_2 \prod_{i=1}^{3} \frac{1}{z-E_i-R_i(z)}
\end{aligned} \tag{2.51}$$

where we have labeled:

$$\begin{aligned}
E_1 &= E_u & R_1(z) &= \textstyle\sum_{k_j} \frac{|g_1|^2}{z-k_j-E_x} \\
E_2 &= k_1 + E_x & R_2(z) &= \textstyle\sum_{k_i} \frac{|g_2|^2}{z-k_1-k_j} \\
E_3 &= k_1 + k_2 & R_3(z) &= 0
\end{aligned} \tag{2.52}$$

As before, we use Eq. 2.36 to write for $i = 1, 2$

$$R_i(z) = \Upsilon_i(z) - i\Gamma_i(z), \tag{2.53}$$

where, as in the previous subsection,

$$\Upsilon_i(z) = \fint \frac{|g_i|^2}{Re(z)-k-E_x} dk \tag{2.54}$$

$$\Gamma_i(z) = \pi |g_i|^2 \tag{2.55}$$

We can substitute Eqs. 2.51-2.54 back in the expression for the evolution operator, Eq. 2.4 and write:

$$\langle k_1,k_2;d| U(t) |0;u\rangle = \frac{g_1 g_2}{2\pi i} \int dz e^{-izt} \prod_{i=1}^{3} \frac{1}{z-(E_i+\Upsilon_i)+i\Gamma_i}, \tag{2.56}$$

where the intergration is along I_+. We can deform the contour in the same procedure as the previous section. The integral has now contributions from three poles and from the integral on the sides of the cut. We discard the contributions from the two poles which are not on the real axis and from the branch cut integral for the same reasons and calculations as in the previous subsection. That is, the contribution to the integral is solely from the pole on the real axis $z = k_1 + k_2$:

$$\begin{aligned}\langle k_1, k_2; d| U(t) |0; u\rangle &= g_1 g_2 e^{-i(k_1+k_2)t} \frac{1}{k_1 + k_2 - (E_x + k_1 + \Upsilon_x) + i\Gamma_i} \frac{1}{k_1 + k_2 - (E_u + \Upsilon_u) + i\Gamma_u} \\ &= e^{-i(k_1+k_2)t} \frac{g_2}{k_2 - E_x + i\Gamma_x} \frac{g_1}{k_1 + k_2 - E_u + i\Gamma_u} \end{aligned} \tag{2.57}$$

We have redefined the energies to include the Lamb shift Υ_i. We can also write this in the form

$$\langle k_1, k_2; d| U(t) |0; u\rangle = e^{-i(k_1+k_2)t} A(k_2, Z_x) A(k_1 + k_2, Z_u), \tag{2.58}$$

where we have used the definition of $A(k, z)$ as appeared in Eq. 2.44. If we define:

$$\alpha_x \triangleq A(k_2, Z_x) A(k_1 + k_2, Z_u), \tag{2.59}$$

then Eq. 2.58 is written

$$\langle k_1, k_2; d| U(t) |0; u\rangle = e^{-i(k_1+k_2)t} \alpha_x \tag{2.60}$$

Thus we have found the amplitude of the emitted photons from a three levels radiative cascade.

2.6 Quadrilateral model

Let us now consider the quantum dot model. We restrict ourselves to the subspace of three excitations, as in the previous section. The summation in Eq. 2.24 is over the levels x, y, d, u (the system is shown in Fig. 1) and the interaction V is given by:

$$V = \sum_{k_1,\varepsilon} g_{1,\varepsilon} |k_1; \varepsilon; \hat{\boldsymbol{\varepsilon}}\rangle \langle 0; u| + \sum_{k_1,k_2,\varepsilon} g_{2,\varepsilon} |k_1, k_2; d; \hat{\boldsymbol{\varepsilon}}\rangle \langle k_1; \varepsilon; \hat{\boldsymbol{\varepsilon}}| \tag{2.61}$$

The difference between this equation and Eq. 2.46 in the three levels model is the additional polarization index ε. When it appears in the second slot, it represents the intermediate states, $\varepsilon = x, y$. The additional (third) slot represents the polarization of the photons (when there exist photons) and in this case $\hat{\boldsymbol{\varepsilon}} = \hat{\mathbf{x}}, \hat{\mathbf{y}}$.

We need to refine our definition in Eq. 2.25, to include the polarization of the photons. P_n^{ε} is now the projector on the subspace which contains n photons with $\hat{\boldsymbol{\varepsilon}}$ polarization, for example:

$$P_2^y \triangleq \sum_{k_i,k_j} |k_i, k_j; d; \hat{\mathbf{y}}\rangle \langle k_i, k_j; d; \hat{\mathbf{y}}| \tag{2.62}$$

In our model, we exclude the subspace with one $\hat{\mathbf{x}}$ polarized photon and one $\hat{\mathbf{y}}$ polarized photon due to the fact that the radiative cascade can only generate photons with either both $\hat{\mathbf{x}}$ polarization or both $\hat{\mathbf{y}}$ polarization, see Fig. 1. Thus, the identity operator for the subspace of three excitations is:

$$\mathbb{1} = P_0 + P_1^x + P_2^x + P_1^y + P_2^y \tag{2.63}$$

The generalization of the previous section to a four level system as depicted in Fig. 1 is trivial, if we notice that the only linking chain of the x and y cascade is the u level. Formally, the hamiltonian, after the elimination of the upper level, is decomposed to a block matrix, one block for the x channel, the other for the y channel:

$$\begin{aligned}(\mathbb{1} - P_0)H(\mathbb{1} - P_0) &= (P_1^x + P_2^x + P_1^y + P_2^y)H(P_1^x + P_2^x + P_1^y + P_2^y) \\ &= (P_1^x + P_2^x)H(P_1^x + P_2^x) + (P_1^y + P_2^y)H(P_1^y + P_2^y)\end{aligned} \tag{2.64}$$

This results in

$$G(V, \mathbb{1} - P_0; z) = G(V, P_1^x + P_2^x; z) + G(V, P_1^y + P_2^y; z) \tag{2.65}$$

Since, for $\varepsilon \neq \varepsilon'$

$$\langle k_1, k_2; d; \hat{\boldsymbol{\varepsilon}}|\, G(V, P_1^{\varepsilon'} + P_2^{\varepsilon'}; z) = 0 \tag{2.66}$$

We get

$$\langle k_1, k_2; d; \hat{\boldsymbol{\varepsilon}}|\, G(V, \mathbb{1} - P_0; z) = \langle k_1, k_2; d; \hat{\boldsymbol{\varepsilon}}|\, G(V, P_1^{\varepsilon} + P_2^{\varepsilon}; z) \tag{2.67}$$

Using this with Eqs. (2.15, 2.36) and following the same procedure as in the previous subsections we obtain:

$$\begin{aligned}\langle k_1, k_2; d; \hat{\boldsymbol{\varepsilon}}|\, G(z)\,|u\rangle &= \langle k_1, k_2; d; \hat{\boldsymbol{\varepsilon}}|\, G(V, P_2^{\varepsilon} + P_1^{\varepsilon}; z) V G(R^{1-P_0}, P_0; z)\,|0; u\rangle \\ &= \langle k_1, k_2; d; \hat{\boldsymbol{\varepsilon}}|\, G(0, P_2^{\varepsilon}; z) V G(R^{P_2^{\varepsilon}}, P_1^{\varepsilon}; z) \mathbb{1} V \mathbb{1} G(R^{1-P_0}, P_0; z)\,|0; u\rangle \\ &= \langle k_1, k_2; d; \hat{\boldsymbol{\varepsilon}}|\, G(0, P_2^{\varepsilon}; z) V G(R^{P_2^{\varepsilon}}, P_1^{\varepsilon}; z) P_1^{\varepsilon} V P_0 G(R^{1-P_0}, P_0; z)\,|0; u\rangle \\ &= \sum_{k_i} \langle k_1, k_2; d; \hat{\boldsymbol{\varepsilon}}|\, G'(0, P_2^{\varepsilon}; z) V G'(R^{P_2^{\varepsilon}}, P_1^{\varepsilon}; z)\,|k_1; \varepsilon; \hat{\boldsymbol{\varepsilon}}\rangle \langle k_1; \varepsilon; \hat{\boldsymbol{\varepsilon}}|\, V\,|0; u\rangle \\ &\quad \times \langle 0; u|\, G'(R^{1-P_0}, P_0; z)\,|0; u\rangle\end{aligned} \tag{2.68}$$

This form is similar to the one in Eq. 2.48. The first two terms are just the same as in Eq. 2.48 under the exchange $\varepsilon \leftrightarrow x$. The last term can be expressed as in Eq. 2.49 under $P_i \to P_i^x + P_i^y$, $i = 1, 2$. The R^{1-P_0} expression, Eq. 2.50, is modified to:

$$\begin{aligned}\langle 0;u|\, R^{P_1+P_2}\,|0;u\rangle &= \langle 0;u|\, V(P_1^x+P_1^y)\frac{1}{z-(P_1^x+P_1^y)H_0(P_1^x+P_1^y)}(P_1^x+P_1^y)V\,|0;u\rangle \\ &= \langle 0;u|\, VP_1^x\frac{1}{z-P_1^xH_0P_1^x}P_1^xV\,|0;u\rangle + \langle 0;u|\, VP_1^y\frac{1}{z-P_1^yH_0P_1^y}P_1^yV\,|0;u\rangle \\ &= \sum_{k_j}\frac{|g_{1,x}|^2}{z-k_j-E_x}+\sum_{k_j}\frac{|g_{1,y}|^2}{z-k_j-E_y} \end{aligned} \tag{2.69}$$

We have used the fact that P_1^x and P_1^y are projections on different eigenspaces of H_0, and $P_1^xVP_1^y = 0$. Thus we obtain:

$$\langle k_1,k_2;d;\hat{\boldsymbol{\varepsilon}}|\, G(z)\,|u\rangle = \langle k_1,k_2;d;\hat{\boldsymbol{\varepsilon}}|\, V\,|k_1;x;\hat{\boldsymbol{\varepsilon}}\rangle\,\langle k_1;x;\hat{\boldsymbol{\varepsilon}}|\, V\,|0;u\rangle\prod_{i=1}^{3}\frac{1}{z-E_i-R_i^{\varepsilon}(z)} \tag{2.70}$$

where, similar to the definitions of Eq. 2.52

$$\begin{aligned} E_1^{\varepsilon} &= E_u & R_1(z) &= \textstyle\sum_{k_j,\varepsilon}\frac{|g_{1,\varepsilon}(k_j)|^2}{z-k_j-E_x} \\ E_2^{\varepsilon} &= k_1+E_{\varepsilon} & R_2(z) &= \textstyle\sum_{k_i}\frac{|g_{2,\varepsilon}(k_i)|^2}{z-k_i} \\ E_3^{\varepsilon} &= k_1+k_2 & R_3(z) &= 0 \end{aligned} \tag{2.71}$$

Using the same approximations, we integrate along the contour which was described in the previous subsections and depicted in Fig. 4. The integral is approximated by the contribution from the pole on the real axis. This yields

$$\begin{aligned}\langle k_1,k_2;d;\hat{\boldsymbol{\varepsilon}}|\, U(t)\,|0;u\rangle &= \lambda_{\varepsilon}e^{-i(k_1+k_2)t}A(k_2,Z_{\varepsilon})A(k_1+k_2,Z_u) \\ &= \lambda_{\varepsilon}\alpha_{\varepsilon}e^{-i(k_1+k_2)t}, \end{aligned} \tag{2.72}$$

where $A(k,z_j), \alpha_{\varepsilon}$ were defined in Eqs. (2.44,2.59):

$$\begin{aligned} A(k,Z_j) &\triangleq \frac{\sqrt{\Gamma_u/\pi}}{|k|-Z_j}, \quad Z_j = E_j - i\Gamma_j \\ \alpha_{\varepsilon} &\triangleq A(k_2,Z_{\varepsilon})A(k_1+k_2,Z_u) \end{aligned}$$

and

$$\begin{aligned}\lambda_{\varepsilon} &\triangleq \sqrt{\frac{\pi}{\Gamma_u}}\,\langle k_1;x;\varepsilon|\, V\,|0;u\rangle = \frac{\langle k_1;x;\hat{\mathbf{x}}|\, V\,|0;u\rangle}{\sqrt{|\,\langle k_1;x;\varepsilon|\, V\,|0;u\rangle\,|^2+|\,\langle k_1;y;\hat{\mathbf{y}}|\, V\,|0;u\rangle\,|^2}} \\ &= \frac{g_{1,\varepsilon}}{\sqrt{|g_{1,\varepsilon}|^2+|g_{2,\varepsilon}|^2}} \end{aligned} \tag{2.73}$$

Thus, we derived the emitted photon state, as appeared in Eq. (2.1), as a superposition of the two possible polarizations:

$$|\psi_2(t)\rangle = \sum_{\varepsilon=x,y} \int dk_1 dk_2 \lambda_\varepsilon \alpha_\varepsilon(k_1,k_2) e^{-i(k_1+k_2)t} \; |k_1,k_2\rangle \otimes |\hat{\boldsymbol{\varepsilon}}\hat{\boldsymbol{\varepsilon}}\rangle \tag{2.74}$$

The photons' wave function, is necessarily symmetric, $\alpha_\varepsilon(k_1,k_2) = \alpha_\varepsilon(k_2,k_1)$.

$$\alpha_\varepsilon(k_1,k_2) = \frac{1}{2}\big(A(k_1,Z_\varepsilon) + A(k_2,Z_\varepsilon)\big)A(k_1+k_2,Z_u) \tag{2.75}$$

In the case that the two photons are distinguished by their energies one may forget about the symmetrization and replace Eq. (2.75) by

$$\alpha_\varepsilon(k_1,k_2) = A(k_2,Z_\varepsilon)A(k_1+k_2,Z_u) \tag{2.76}$$

In this case the α's are automatically normalized

$$\langle \alpha_\varepsilon | \alpha_\varepsilon \rangle = 1\,. \tag{2.77}$$

In what follows we shall restrict ourselves to this case.

3 The polarization density matrix and entanglement distillation

In the previous section we have derived the emitted photons state in our specific configuration (quadrilateral model, Fig. 1),

$$|\psi_2(t)\rangle = \sum_{\varepsilon=x,y} \int dk_1 dk_2 \lambda_\varepsilon \, \alpha_\varepsilon(k_1,k_2) e^{i(|k_1|+|k_2|)t} \; |k_1,k_2\rangle \otimes |\hat{\boldsymbol{\varepsilon}}\hat{\boldsymbol{\varepsilon}}\rangle \tag{3.78}$$

where

$$\begin{aligned} \alpha_\varepsilon &\triangleq A(k_2,Z_\varepsilon)A(k_1+k_2,Z_u) \\ A(k,Z_j) &\triangleq \frac{\sqrt{\Gamma_u/\pi}}{|k|-Z_j}, \quad Z_j = E_j - i\Gamma_j \end{aligned} \tag{3.79}$$

and λ_j are the branching ratios, given in Eq. 2.73.

In order to obtain the polarization density matrix, one need to trace out the remaining degrees of freedom of the photons, that is, trace over the wavevectors. Given the 2-photon state, Eq. (2.1), the polarization density matrix ρ is defined by

$$\rho = Tr_{k_1k_2} |\psi_2\rangle \langle\psi_2| \tag{3.80}$$

where the partial trace is over the two photons' wave numbers k_j.

The reduced polarization density matrix is given by a 4×4 density matrix. In our configuration, the intermediate levels $\varepsilon = x, y$ dictate the polarization of the photons so that in one arm the two photons are $\hat{\mathbf{x}}$ polarized and in the second the two are $\hat{\mathbf{y}}$ polarized. The resulting density matrix has only 4 non-zero entries (instead of 16 in general) and is of the form

$$\rho = \begin{pmatrix} \rho_{xx} & 0 & 0 & \rho_{xy} \\ 0 & 0 & 0 & 0 \\ 0 & 0 & 0 & 0 \\ \bar{\rho}_{xy} & 0 & 0 & \rho_{yy} \end{pmatrix} \tag{3.81}$$

written in the basis $|\hat{\mathbf{x}}\hat{\mathbf{x}}\rangle, |\hat{\mathbf{x}}\hat{\mathbf{y}}\rangle, |\hat{\mathbf{y}}\hat{\mathbf{x}}\rangle, |\hat{\mathbf{y}}\hat{\mathbf{y}}\rangle$ where $\bar{\rho}$ denotes complex conjugation.

As a measure of the entanglement, we take $|\rho_{xy}|$, which is the maximum eigenvalue of the violation of the Peres separability criterion [7, 8]. Assuming $|\lambda_x| = |\lambda_y| = 1/2$ the off

diagonal entry may be computed from Eqs. 3.78-3.79

$$|\rho_{xy}| = \left|\bar{\lambda}_y \lambda_x \langle \alpha_x | \alpha_y \rangle\right| = \left|\bar{\lambda}_y \lambda_x \int dk_1 dk_2 \alpha_y \alpha_x^*\right| = \left(\frac{\Gamma^2}{4(\Delta^2+\Gamma^2)}\right)^{\frac{1}{2}} \tag{3.82}$$

where $\Delta = E_y - E_x$ is the detuning between the intermediate states. It is clear that when $\Delta \gg \Gamma$ the non-diagonal element is small and the entanglement is destroyed. In biexciton decay [9] this is usually the case and and the hierarchy of energy scales is

$$\Gamma_\varepsilon \ll \Delta \ll E_u - E_\varepsilon, E_\varepsilon \ , \quad \varepsilon = x, y \tag{3.83}$$

where the scale of Δ is determined by the electron-hole anisotropic exchange interaction [10, 11].

Physically, this situation describes the state when the "which path" ambiguity is resolved by the different colors of the emitted photons. This essentially kills the entanglement.

However, The entanglement may be distilled by selecting only those photons which possess the "which path ambiguity" [1]. Such photons are those with same probability to be emitted in either the x decay channel or the y decay channel. These photons have the (intermediate) energies $k_1 \approx E_u - \frac{1}{2}(E_x + E_y)$, $k_2 \approx \frac{1}{2}(E_x + E_y)$, as can be seen from Fig. 5 or from Eqs. 3.78-3.79. In practice, the distillation is done by filtering the photons through a spectral *window function*. The photons are detected only if their energy is within a window of width w centered at $E_u - \frac{1}{2}(E_x + E_y)$ for the first photon in the cascade and at $\frac{1}{2}(E_x + E_y)$ for the second one (Fig. 5). This can be implemented experimentally by using a monochromator (or an energy filter) which transmits only a selected part of the emission spectrum, as was demonstrated in Akopian *et al.* [1].

Let $W^2 = W$ be the projections, associated with this spectral filtering. We'll use a specific form for the spectral filter as was mentioned in the previous paragraph, namely

$$\langle k_1, k_2 | W | k_i, k_j \rangle = \delta_{1,i}\delta_{2,j} w(k_1, k_2) \tag{3.84}$$

$$w(k_1, k_2) = \begin{cases} 1 & \left|k_1 - \left(E_u - \frac{E_x+E_y}{2}\right)\right| < w \quad and \quad \left|k_2 - \left(\frac{E_x+E_y}{2}\right)\right| < w \\ 0 & otherwise \end{cases}$$

The identity $W = 1$ ($w = \infty$) represents no filtering.

The distillation produces the (normalized) filtered state

$$\left|\psi_2^f\right\rangle = \frac{W|\psi_2\rangle}{\sqrt{p_w}}, \tag{3.85}$$

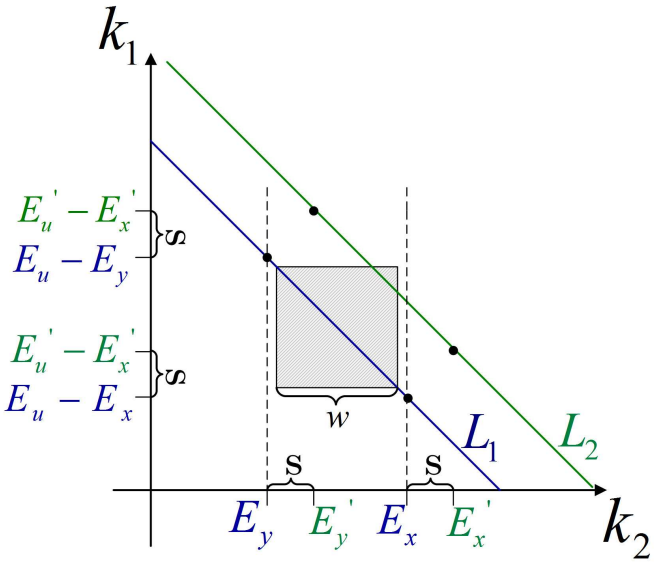

Figure 5: The square represents the spectral filtering. Only wave numbers (k_1, k_2) in the square are retained. The amplitude is most significant near the diagonal line L_1, along which the energy of the two photons adds up to the initial energy ($k_1 + k_2 = E_u$). E_x and E_y are the energies of the intermediate states. As discussed later on in Sec. 5, s describes the slow drift of the levels. The line L_2 obeys the equation $k_1 + k_2 = E_u + 2s$.

with probability $p_w = \langle\psi_2| W |\psi_2\rangle$. The filtered state gives rise to a filtered density matrix ρ^f which is, in general, substantially entangled, i.e. ρ^f_{xy} is significant [1].

The entries in the filtered, or distilled, density matrix of Eq. 3.81 can now be computed from

$$\rho^f_{\varepsilon'\varepsilon} = \frac{\bar{\lambda}_{\varepsilon'}\lambda_\varepsilon}{p_w}\langle\alpha_{\varepsilon'}| W |\alpha_\varepsilon\rangle \tag{3.86}$$

where α_ε is given by Eqs. 3.78-3.79. The normalization p_w may be fixed a-posteriori by normalizing the trace, or, equivalently, is given by the normalization in Eq. (3.85).

The drawback of the distillation process is that the probability to detect the emitted photons is decreases ($p_w < 1$). From Eq. 2.75 it can be seen that the largest contribution to the amplitude is along the intersection of the energy conservation line $k_1 + k_2 = E_u$ with the line $k_2 = E_x$ or the line $k_2 = E_y$. The intersection of the latter lines with the energy conservation line is at the points $(k_1, k_2) = (E_u - E_\varepsilon, E_\varepsilon), \quad \varepsilon = x, y$ as can be seen in Fig. 6. As the filter is narrowed, the entanglement increases and the detection probability decreases. The contribution to the amplitude falls on a scale of $O(\Gamma)$. The magnitude of the off-diagonal element (and hence the entanglement) is set by the two ratios Δ/Γ and w/Γ. However, it is not clear how these parameter effect the phase of the non-diagonal element. This will be discussed in the next section.

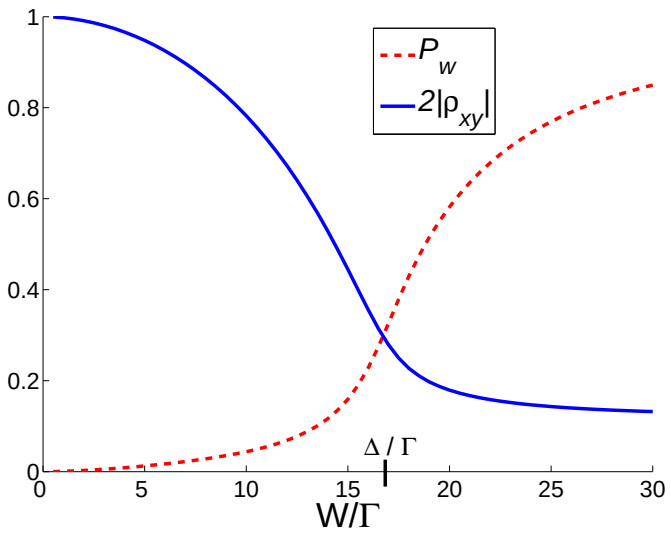

Figure 6: The photon's detection probability p_w and twice the entanglement measure $|2\rho_{xy}|$, where ρ_{xy} is the off-diagonal element. The plot was drawn for $\Delta/\Gamma \approx 17$, as in Akopian *et al* [1]. For $w \to 0$ the asymptotic values are $|2\rho_{xy}| \to 1$ and $p_w \to 0$ and for $w \to \infty$ the asymptotic values are $|2\rho_{xy}| \to \left(\frac{\Gamma^2}{4(\Delta^2+\Gamma^2)}\right)^{\frac{1}{2}}$ and $p_w \to 1$. The sharp change between these values happens on a scale of $O(\Gamma)$ in the vicinity of the point $w = \Delta$.

4 The phase of the off diagonal element

Before we discuss the off-diagonal element's phase, we rewrite Eq. 3.86 as

$$\begin{aligned} \rho^f_{xy} &= \frac{\bar{\lambda}_x \lambda_y}{p} \langle \alpha_x | \, W \, | \alpha_y \rangle \\ &= \frac{\bar{\lambda}_x \lambda_y g_{2,y} \bar{g}_{2,x}}{p} \langle \alpha_x | \, W \, | \alpha_y \rangle \, (g_{2,y} \bar{g}_{2,x})^{-1} \end{aligned} \tag{4.87}$$

From Eq. 4.87 the phase of the off-diagonal element ρ^f_{yx} may have contributions from both the $\bar{\lambda}_x \lambda_y \bar{g}_{2,x} g_{2,y}$ term and the $\langle \alpha_x | \, W \, | \alpha_y \rangle (\bar{g}_{2,x} g_{2,y})^{-1}$ term, the latter depending on the spectral filter used. In Sec. 4.1 we shall use time reversal and a symmetry argument to show that $\lambda_x \bar{\lambda}_y \bar{g}_{2,x} g_{2,y}$ is a positive quantity. It then follows that the phase of ρ_{xy} is fully determined by the phase of $\langle \alpha_x | \, W \, | \alpha_y \rangle (\bar{g}_{2,x} g_{2,y})^{-1}$. In Sec. 4.2 we will study the dependency of this expression on the various parameters of the system, followed by a discussion of some interesting limiting cases.

4.1 Branching ratios and matrix elements

The branching amplitudes are related to dipole matrix elements that govern the transitions. Each coupling constant, under the dipole approximation, is proportional to such a matrix element as can be seen in Eq. 2.22. There are 4 dipole matrix elements, shown in Fig. 1, denoted by M_ε^ℓ where $\ell = u, d$ and $\varepsilon = x, y$, namely

$$M_x^\ell = \langle x| \mathbf{X} |\ell\rangle , \quad M_y^\ell = \langle y| \mathbf{Y} |\ell\rangle , \quad \ell = d, u \tag{4.88}$$

with $\mathbf{X}$ the (possibly second quantized) x-position operator, and similarly for $\mathbf{Y}$.

As $E_x \approx E_y$ (the difference is on the scale of Γ, which is the small parameter), the coefficients of the dipole matrix elements, M_j^ℓ, in Eq. 2.22 are the same for $\varepsilon = x$ and $\varepsilon = y$. From Eqs. (2.72-2.74) the branching amplitudes are proportional to the appropriate product of dipole matrix elements. This allows us to write Eq. 3.79 as

$$|\psi_2(t)\rangle = \sum_{\varepsilon=x,y} C M_\varepsilon^u M_d^\varepsilon \int dk_1 dk_2 f_\varepsilon(k_1, k_2) e^{i(|k_1|+|k_2|)t} \; |k_1, k_2\rangle \otimes |\hat{\boldsymbol{\varepsilon}}\hat{\boldsymbol{\varepsilon}}\rangle \tag{4.89}$$

where C is a common constant and $f_j(k_1, k_2)$ is a function of k_1, k_2:

$$f_\varepsilon(k_1, k_2) = \frac{1}{|k_2| - Z_\varepsilon} \frac{1}{|k_1 + k_2| - Z_u} \tag{4.90}$$

It follows that

$$\rho_{xy}^f = |C|^2 M_y^u M_d^y \bar{M}_x^u \bar{M}_d^x \int dk_1 dk_2 \; w(k_1, k_2) \bar{f}_x(k_1, k_2) f_y(k_1, k_2) \tag{4.91}$$

In this section we will show that the product of dipole elements

$$D = M_y^u M_d^y \bar{M}_x^u \bar{M}_d^x = M_y^u M_y^x M_x^d M_u^x \tag{4.92}$$

is in general real, and in our case positive. In the next section the integral will be discussed. Observe, first, that this quantity is independent of the gauge choice of the radiating system states $|j\rangle$, as every ket is paired with the corresponding bra (the up-down indices are paired). We will now show that time-reversal implies that the product of dipole matrix elements is real.

Let T denote the antiunitary operator associated with time reversal [12, 13], i.e.

$$\langle Tj|Tk\rangle = \langle k|j\rangle$$

In the non-degenerate case $T|j\rangle = e^{i\gamma}|j\rangle$, where γ is a gauge dependent angle. By changing the gauge to $|j\rangle \to e^{i\gamma/2}|j\rangle$, one then sees that $|j\rangle$ may be chosen so that

$T|j\rangle = |j\rangle$. Recall that the components of the position operator $\mathbf{X}$ and $\mathbf{Y}$, (possibly second quantized) are even under time reversal so $T^\dagger \mathbf{X} T = \mathbf{X}$. Plugging this in the definition of the dipole matrix elements we see that

$$\langle \ell | \mathbf{X} | \varepsilon \rangle = \langle \ell | T^\dagger \mathbf{X} T | \varepsilon \rangle = \langle T\ell | \mathbf{X} | T\varepsilon \rangle = \langle \varepsilon | \mathbf{X} | \ell \rangle$$

and similarly[3] for $\mathbf{Y}$. This says that there is a choice of gauge that makes all dipole matrix elements real. However, as we have noted D is independent of the choice of gauge and so is real irrespective of how one chooses the eigenfunctions.

We are left with the sign ambiguity of D in Eq. (4.91). This sign is not a function of the window width w (a parameter on the experimental system) but could, in principle, depend on the level's configuration, including the parameter Δ. Assuming that the sign is continuous it is enough to determine the sign at a single point for the following reason. Each other point can be connected to that specific point by a smooth curve. The sign of the product of dipole matrix elements changes continuously with the Hamiltonian of the system. Since the product $|C|^2 M_x^u M_d^x M_y^d M_u^y$ is nonzero and real (if the product were zero, then at least one of the transitions in Fig. 1 would be ruled out), the other point has the same sign. We shall now present an argument that allows to determine the sign on the line $\Delta = 0$.

The case $\Delta = 0$ represents exact degeneracy. Assume that the degeneracy is a consequence of rotational symmetry in the x-y plane of the radiating system (this is the case in quantum dots). As the initial state u is not degenerate, it must be a state of angular momentum 0 about the z-axis. Since angular momentum is conserved the final two photon state must also be a state of zero angular momentum about the z-axis.

To find a representation of zero angular momentum for the two photon states we proceed as follows: Let $i\sigma_y$ denote the operator (in the computational basis) that takes the x polarization to the y polarization:

$$i\sigma_y |x\rangle = |y\rangle\,, \quad i\sigma_y |y\rangle = -|x\rangle \tag{4.93}$$

Rotation by α of the 2-photon pair is then implemented by $e^{i\alpha\sigma_y} \otimes e^{i\alpha\sigma_y}$. Hence the operator of total angular momentum about the z-axis (i.e. the generator of joint rotations) of the photon pair is

$$\mathbb{I} \otimes \sigma_y + \sigma_y \otimes \mathbb{I} \tag{4.94}$$

The eigenvectors with zero total angular momentum of this operator are, by direct calcu-

[3]For the cascade in question $\langle \ell | \mathbf{X} | y \rangle = \langle \ell | \mathbf{Y} | x \rangle = 0$.

lation,

$$\frac{|xx\rangle + |yy\rangle}{\sqrt{2}}, \quad \frac{|xy\rangle - |yx\rangle}{\sqrt{2}} \tag{4.95}$$

Comparison with Eq. (2.1) shows that only the first vector is relevant and fixes $\lambda_\varepsilon = 1/\sqrt{2}$ up to an overall phase. It follows that with full rotational symmetry $\lambda_x \bar{\lambda}_y = \frac{1}{2}$. By continuity the sign of D is then positive, and the sign ambiguity is resolved.

4.2 The role of the complex pole

It follows from the previous subsection and Eq. 4.91 that the off-diagonal elements in the density matrix is proportional to $\langle \alpha_x | W | \alpha_y \rangle$. This is determined by a two-dimensional integration of the function

$$w(k_1, k_2) \left| \frac{1}{|k_1| + |k_2| - Z_u} \right|^2 \frac{1}{|k_2| - Z_y} \frac{1}{|k_2| - \bar{Z}_x} \tag{4.96}$$

The first two factors are positive, and the role they play is to weigh the integrand. The positive factor $\left| |k_1 + k_2| - Z_u \right|^{-2}$ may be interpreted as guaranteeing approximate conservation of total energy since

$$\lim_{\Gamma \to 0} \left| \frac{1}{|k_1| + |k_2| - Z_u} \right|^2 = \delta(|k_1| + |k_2| - E_u) \tag{4.97}$$

This means that to leading order in Γ the matrix elements of ρ are determined by a one-dimensional integral over k of the function

$$w(E_u - k_2, k_2) \frac{1}{|k_2| - Z_y} \frac{1}{|k_2| - \bar{Z}_x} = w(E_u - k_2, k_2) \frac{|k_2| - \bar{Z}_y}{\left||k_2| - Z_y\right|^2} \frac{|k_2| - Z_x}{\left||k_2| - \bar{Z}_x\right|^2} \tag{4.98}$$

In particular, the phase of the off-diagonal element ρ_{xy} is therefore essentially governed by the phases of $(|k_2| - \bar{Z}_y)(|k_2| - Z_x)$. This is represented graphically in Fig. 7 by the arrows that point from the point k_2 to the resonance energies Z_x and $\bar{Z}_y$. This procedure, outlined above, reduces the computation of the density matrix to integration. In general, this may be carried out only numerically. There are certain limiting cases, however, that can be analyzed by inspection.

Strong filtering:

Suppose the filtering window W is very narrow with width $w \ll \Delta$ and is centered at $\frac{1}{2}(E_x + E_y)$ and $E_u - \frac{1}{2}(E_x + E_y)$. The detuning is much larger than the radiative width

$\Delta \gg \Gamma$. The window restricts the domain of integration and one finds that the detection probability is small and scales linearly with the window's width $p_w = O(\frac{w\Gamma}{\Delta^2})$. The phase of the off-diagonal element is $\pi - 4\Gamma/\Delta$ and its magnitude is approximately,

$$\rho_{xy} = \frac{1}{2} - O\left(\frac{\Gamma}{2\Delta}\right) \tag{4.99}$$

The state is close to a maximally entangled state.

As the change in these proprties happens on a scale of $O(\Gamma)$ near $\Delta = w$ (Fig. 6), these approximations are appropriate when $\Delta - w \geq O(\Gamma)$. This gives the upper left triangle of Fig. 8 and the left part of Fig. 6.

No filtering:

No filtering corresponds to $W = 1$ and a width $w = \infty$. In these case, $p_w = 1$. With exact degeneracy $\Delta = 0$ the state is maximally entangled, $\rho_{xy} = 1/2$. The two arrows in Fig. 7 are complex conjugates so the phase of ρ^f_{xy} is 0.

When $\Delta \gg \Gamma$ the integrals are dominated by the neighborhood of the poles at $k = E_x, E_y$. One finds by explicit integration that the magnitude is small and given in Eq. 3.86. The off-diagonal element is almost purely imaginary and $\rho^f_{xy} = O\left(i\frac{\Gamma}{Z_y - Z_x}\right)$. This accounts for the lower right hand triangle of the figure $[w - \Delta \geq O(\Gamma)]$ and the right hand part of Fig. 6.

When $\Delta \to \infty$ it is easy to see that $\rho^f_{xy} \to 0$. The off diagonal term vanishes and its phase is ill defined at the top-right corner of Fig. 8.

(a)

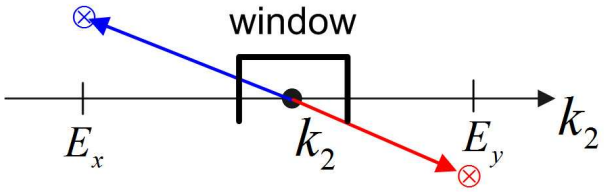

(b)

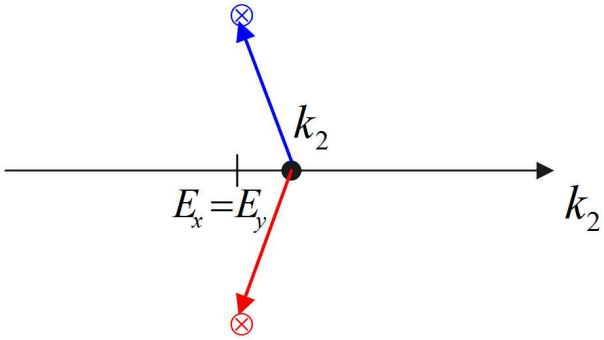

(c)

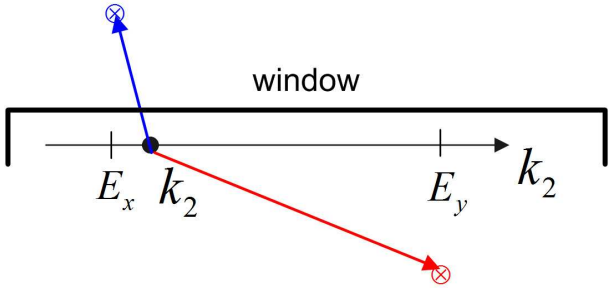

Figure 7: The phase of the integrand is determined by the product of the two complex numbers, represented as arrows, pointing from k_2 to the location of the complex energies Z_ε (blue arrow for Z_x and red arrow for Z_y). The location of k_2 is restricted by the window function W. In figure (a) the levels are detuned and the spectral window is smaller than the detuning. In figure (b) the levels are degenerate and in figure (c) the levels are detuned and the window is larger than the detuning.

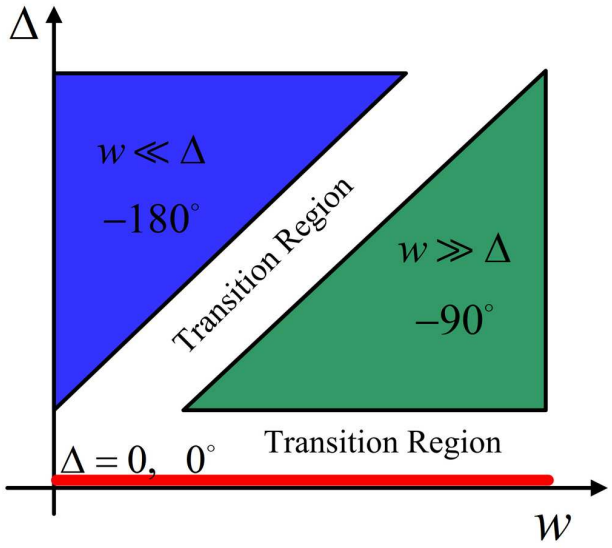

Figure 8: A "phase diagram" for the phase of the off-diagonal element in the density matrix ($\arg(\rho_{xy})$). The widths of transition regions are proportional to the radiative width Γ which is the smallest energy scale in the problem.

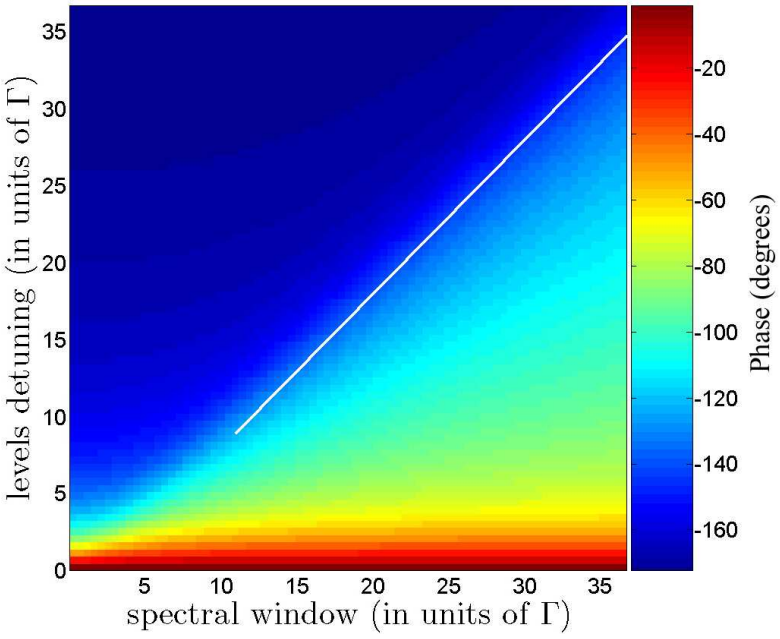

Figure 9: The phase of ρ^f_{xy} as a function of the (centered) normalized spectral window width w/Γ and the detuning Δ/Γ. The line obeys the equation $w = \Delta - 2\Gamma$. For $w, \Delta \gg \Gamma$, for any w which is smaller than $\Delta - 2\Gamma$ the phase does not change appreciably and it is close to 180°.

5 Application to quantum dots

Radiative cascades with partial ambiguity in their decay path information, such as the ones illustrated in Fig. 1, are found naturally in semiconductor quantum dots. In these systems the excited state $|u\rangle$ is associated with a biexciton state, the states $|x\rangle$ and $|y\rangle$ are the intermediate excitonic states, while the state $|d\rangle$ refers to an empty quantum dot. Thereby, the discussion above could in principle be applied straightforwardly to photons emitted from these quantum dots. These systems present, however, yet another complication, as their energies may slowly fluctuate on a time scale much longer than $1/\Gamma$. These fluctuations are caused by electrostatic changes in the semiconductor hosting the quantum dots. In typical cases [1], the fluctuations in the energies are large, with full width at half-maximum (FWHM) comparable or even larger than Δ.

One may worry that these fluctuations may hinder a distillation based on fixed spectral windows. For example, the energy of one of the decay channels can drift into the spectral window while the other does not (or even gets further removed from the window). However, as we show below, under reasonable assumptions, the filtering process is protected so that the magnitude and the phase of the off diagonal element of the actually measured density matrix are only slightly affected by these fluctuations.

Generally, suppose that the energies of the radiative cascade are described by random variables s, with measure $dP(s)$. These in turn give a filtered, probabilistic density matrix $\rho^f(s)$. One is interested in the average density matrix $\left\langle \rho^f \right\rangle$ that characterizes the mixtures of density matrices that are obtained this way. For a given window and a given value of s, the probability to measure the density matrix $\rho^f(s)$ is $Tr(W\rho(s))$. Hence, the expected density matrix is

$$\left\langle \rho^f \right\rangle = \int dP(s)\, Tr(W\rho(s))\, \rho^f(s) = \int dP(s)\, Tr_{k_1 k_2} \left(W \left|\psi_2(s)\right\rangle \left\langle\psi_2(s)\right| W\right)$$

If one assumes that the drift is caused by meandering local potential, the biexciton is affected twice as much as the exciton, since the biexciton energy is given by $E_u = 2E_x + \Delta/2 - B$, where B is the biexciton binding energy[14]. The biexciton binding energy is typically more than two orders of magnitude smaller than the exciton energy and its dependence (as well as that of the detuning, Δ) on local electrostatic fields can be safely ignored. This can be verified experimentally by the application of an external field [15]. Therefore, one random variable s describes the shift of all the relevant energy levels by

$$E_x \to E_x^{'} \triangleq E_x + s, \quad E_y \to E_y^{'} \triangleq E_y + s, \quad E_u \to E_u^{'} \triangleq E_u + 2s \tag{5.100}$$

With this model in mind, we review the consequences of the spectral drift on the magnitude and phase of the off diagonal element of the density matrix. The spectral filter filters both photons within an energy window of width w, as represented by a square in the space k_1, k_2 in Fig. 5. The largest contributions to the integrals arise from points close to the intersection of the line $E_u = k_1 + k_2$ with the pole lines $k_2 = E_x$ and $k_2 = E_y$. The spectral window is set such that for no spectral drift, $s = 0$, these points lie close to the corners of the square in Fig. 5 with $w \lesssim \Delta - 2\Gamma$, such that the non-diagonal elements of the density matrix have significant magnitude.

For $s \neq 0$ Eq. (5.100) implies that the intersection points move in the direction $\hat{\mathbf{k_1}}$ a distance s and likewise in the direction $\hat{\mathbf{k_2}}$, as shown in Fig. 5. This means that the probability $Tr(W\rho^f(s))$ of detecting a photon pair decreases rapidly with increasing $|s|$, as the intersection of the energy conservation line with the spectral filter box is getting shorter. Hence we conclude that for large s the contribution of $\rho^f(s)$ is small due to the attenutation of both $Tr(W\rho^f(s))$, the probability to detect photons in such configuration and $dP(s)$, the probability to get such a configuration in the first place.

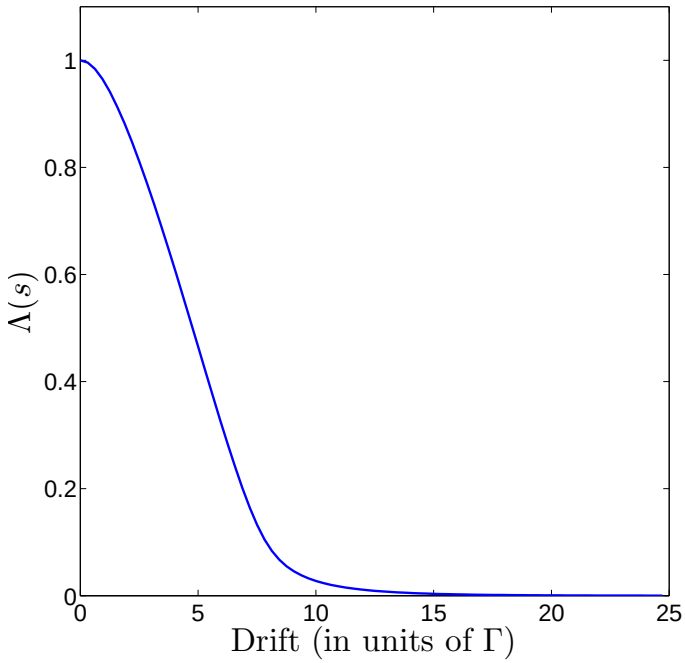

Figure 10: The relative "weight" of the density matrix $\rho(s)$. The weight is given by $\Lambda(s) = P(s)Tr(W\rho(s))$. The plot is renormalized to yield $\Lambda(s = 0) = 1$. The plot is obtained with the experimental values as in Sec. 6.

6 Comparison with experiment

We now turn to compare the theoretical calculation with the experimental data as described by Akopian et al. [1]

The parameters used in the theory were measured independently[4]: $\Gamma_x \approx \Gamma_y = 0.8 \pm 0.2[\mu eV]$, $\Gamma_u \approx 2\Gamma_x$ and $E_x \approx E_y = 1.28[eV]$, $E_u = 2.55[eV]$, $\Delta = 27 \pm 3[\mu eV]$. The window that was used in the experiment was of width $w = 25 \pm 10[\mu eV]$.

The distribution $P(s)$ of the spectral shift was evaluated from the measured spectral lines. It was rather wide, with full width middle height of about $50[\mu eV]$. With the values listed above the probability of detection $Tr(W\rho(s))$ falls much faster than the distribution $P(s)$ as a function of $|s|$, to half its value at $|s| \sim 4[\mu eV]$.

The numerically calculated contribution to $\langle \rho^f \rangle$ (*i.e.* probability of detection times probability distribution for s) as a function of the spectral drift s for the above parameters is displayed in Fig. 10.

When we come to compare the theory with the experimental results, we must take into account the errors of the measurement of the density matrix of the photons, as well as the errors on the parameters Δ, Γ,s and w. These are displayed in Fig. 11. The measured phase in the experiment was $-110^\circ \pm 17^\circ$ where we have taken into account the effect of the beam splitter. The beam splitter induces a phase shift of 180° between the X and Y polarizations of the reflected photon only (this was ignored in Akopian et al. [1], where the phase was 70°). This is compared to the theoretical result $-160^\circ \pm 45^\circ$, which shows a good fit with the experiment.

[4]We are using the half-width at half maximum (HWHM) convention, while in [1, 4] the radiative width is given according to the FWHM convention.

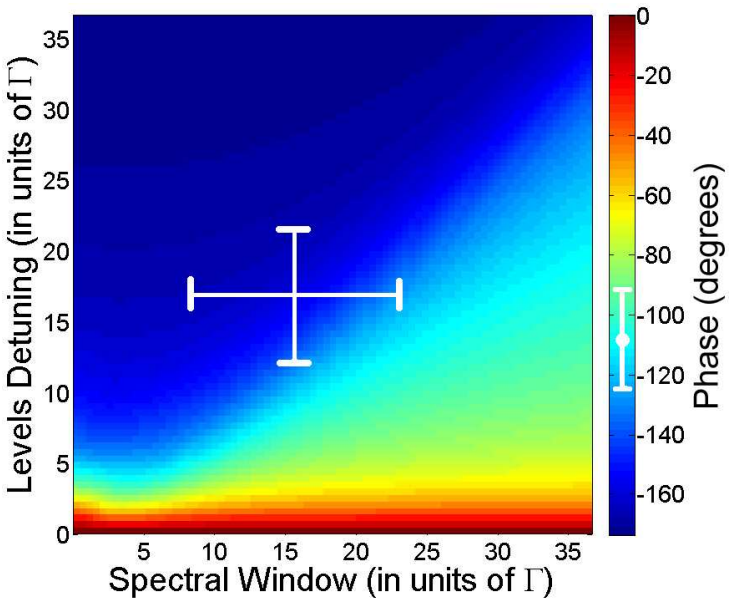

Figure 11: Comparison between the experimental results of Akopian et al. and the theory. The graph shows a theoretical calculation of the phase as a function of the window, w and the detuning, Δ, both in units of Γ. The calculation uses the experimentally measured parameters w, Δ, Γ and s_0. The uncertainties in these parameters result in an area (rather than a point) indicated by the error bars. The possible theoretical values of the phase are in the area which is bounded by these error bars. These values need to be compared to the experimentally measured phase and error, which is represented in the color bar to the left.

7 Summary and Conclusions

We have shown that a very basic model for the emitted photons from a radiative cascade can yield results which are in good agreement with the theory. The basic model requires phenomenological parameters (the levels energies and the radiative width) and knowledge of the experimental system (for example, the spectral window used). This basic model explains why the spectral filtering which was used in Akopian *et al.* [1] yielded an entangled denisty matrix, while when it was not used the resulting density matrix was not entangled. It also predicts that the non-diagonal element should be complex number, and the phase can be estimated theoretically. The phase contains information on the radiating system and about the measurement system, and the theoretical prediction of the phase fits reasonably with the experimental result.

A Gauge fixing and quantum tomography

Here we discuss how the choice of gauge affects a 2 qubit density matrix. Our goal is to show that once a frame and gauge are fixed, the phases in the density matrix have physical meaning.

Consider first a single polarization qubit. The Bloch sphere of polarizations comes with distinguished points: The equator of linear polarizations and the poles of circular polarizations [16]. To choose a frame, pick an arbitrary point on the equator as the horizontal polarization X. This then defines the antipodal point as the vertical polarization Y. Now that the frame is fixed, there remains a gauge freedom of two phases associated with the two base vectors $|X\rangle$ and $|Y\rangle$.

In the general case where a black box emits a pair of photons in two *different* directions, there are 2 phases reflecting the choice of two frames and 4 phases reflecting the choice of gauges. In the case that both photons are emitted in the same direction, the case we focus on, one may choose the same frame for both photons. Note that changing a frame affects both the magnitudes and phases of the entries in the density matrix. Once the frame is fixed, there are still 4 phases reflecting the choice of gauge. The general gauge transformation is given by

$$e^{i\theta_1 I + i\theta_3\sigma_z} \otimes e^{i\theta_2 I + i\theta_4\sigma_z} \tag{A.101}$$

Two of these phases (θ_1 and θ_2) are associated with gauge transformations which do not affect the density matrix (overall phase). The remaining 2 affect (only) the phases of the density matrix. Therefore, the individual phases of the density matrix are gauge dependent[5] and a choice of gauge must be explicitly specified in order to give them a physical meaning.

Quantum tomography is a method of constructing the density matrix from 16 *actual measurement* made on a state generated by a "black box". However, there is no "canonical" linear-independent set of 16 measurements. To relate different sets one needs to specify frames and gauges.

Thus any quantum tomography procedure say, the one presented by James et al.[17], has a gauge convention built into it. To understand how the frame and gauge fixing come about we first note that the "black box" generating the state comes with an attached coordinate frame with unit vector $\hat{\mathbf{x}}, \hat{\mathbf{y}}, \hat{\mathbf{z}}$. (The frame is assumed to be right handed.) Suppose it emits two photons *both* propagating along the positive $\hat{\mathbf{z}}$ axis. Choose the X

[5]The 6 phases in a 4×4 density matrix depend on the 2 gauge choices θ_3,θ_4. Hence, only 4 relations are gauge invariant

polarization state to coincide with the $\hat{\mathbf{x}}$ axis. For each photon, this fixes $|X\rangle$ up to an overall phase, θ_1 for the first and θ_2 for the second. The state $|Y\rangle$ for each photon is then defined as the $\pi/2$ rotation of $|X\rangle$ about $\hat{\mathbf{z}}$. This fixes $|Y\rangle$, up to *the same* phase ambiguity θ_1 and θ_2, respectively.

These are precisely the two local gauge transformations that do not affect the density matrix. Since we specified explicitly the choice of gauge, we conclude that it is meaningful to consider the physical content of the non diagonal term phase.

References

[1] N. Akopian, N. H. Lindner, E. Poem, Y. Berlatzky, J. Avron, D. Gershoni, B. D. Gerardot, and P. M. Petroff. Entangled photon pairs from semiconductor quantum dots. *Physical Review Letters*, 96(13):130501, 2006.

[2] K. Edamatsu, G. Oohata, R. Shimizu, and T. Itoh. Generation of ultraviolet entangled photons in a semiconductor. *Nature*, 431:167–170, September 2004.

[3] R. J. Young, R. M. Stevenson, P. Atkinson, K. Cooper, D. A. Ritchie, and A. J. Shields. Improved fidelity of triggered entangled photons from single quantum dots. *New Journal of Physics*, 8:29–+, February 2006.

[4] J. Dupont-Roc C. Cohen-Tannoudji and G. Grynberg. *Atom-Photon Interactions*. John Wiley & Sons, 1992.

[5] M. O. Scully and M. S. Zubairy. *Quantum Optics*. Cambridge University Press, 1997.

[6] V. Bach, J. Fröhlich, and I. M. Sigal. Mathematical theory of nonrelativistic matter and radiation. *Letters in Mathematical Physics*, 34:183–201, July 1995.

[7] Asher Peres. Separability criterion for density matrices. *Phys. Rev. Lett.*, 77(8):1413–1415, Aug 1996.

[8] Horodecki R. Violating bell inequality by mixed spin-1/2 states: necessary and sufficient condition. *Physics Letters A*, 200:340–344(5), 1 May 1995.

[9] Grigorii E. Ivchenko, E. L. Pikus. *Superlattices and other heterostructures : symmetry and optical phenomena*. Springer, 2nd edition, 1997.

[10] T. Takagahara. Effects of dielectric confinement and electron-hole exchange interaction on excitonic states in semiconductor quantum dots. *Phys. Rev. B*, 47(8):4569–4584, Feb 1993.

[11] M. Bayer, A. Kuther, A. Forchel, A. Gorbunov, V. B. Timofeev, F. Schäfer, J. P. Reithmaier, T. L. Reinecke, and S. N. Walck. Electron and hole g factors and exchange interaction from studies of the exciton fine structure in $in_{0.60}ga_{0.40}as$ quantum dots. *Phys. Rev. Lett.*, 82(8):1748–1751, Feb 1999.

[12] Robert G. Sachs. *The physics of time reversal*. University of Chicago Press, 1987.

[13] Albert Messiah. *Quantum mechanics*. Amsterdam, 1961.

[14] S. Rodt, A. Schliwa, K. Pötschke, F. Guffarth, and D. Bimberg. Correlation of structural and few-particle properties of self-organized InAs/GaAs quantum dots. *Phys. Rev. B*, 71(15):155325–+, April 2005.

[15] E. Poem, J. Shemesh, I. Marderfeld, D. Galushko, N. Akopian, D. Gershoni, B. D. Gerardot, A. Badolato, and P. M. Petroff. Polarization sensitive spectroscopy of charged quantum dots. *Phys. Rev. B*, 76(23):235304–+, December 2007.

[16] Isaac L. Nielsen, Michael A. Chuang. *Quantum computation and quantum information*. Cambridge University Press, 2000.

[17] Daniel F. V. James, Paul G. Kwiat, William J. Munro, and Andrew G. White. Measurement of qubits. *Phys. Rev. A*, 64(5):052312, Oct 2001.